†Work sponsored by the U. S. National Bureau of Standards.

*In partial fulfillment of the requirements for the D. Sc. degree.

[1]K. H. Jack and S. Wild, Nature 212, 248 (1966).

[2]M. J. Duggin and L. J. E. Hofer, Nature 212, 248 (1966).

[3]E. J. Fasiska and G. A. Jeffrey, Acta Cryst. 19, 463 (1965).

[4]H. Bernas, I. A. Campbell, and R. Fruchart, J. Phys. Chem. Solids 28, 17 (1967).

[5]G. P. Huffman, P. R. Errington, and R. M. Fisher, Phys. Status Solidi 22, 473 (1967).

[6]T. Shinjo, F. Itoh, M. Takaki, Y. Nakamura, and N. Shikazono, J. Phys. Soc. Japan 19, 1252 (1964).

[7]M. Ron, H. Shechter, and S. Niedzwiedz, J. Appl. Phys. 39, 265 (1968); H. Shechter and M. Ron, Nucl. Phys. A109, 588 (1968).

[8]H. Ino, T. Moriya, F. E. Fujita, Y. Maeda, Y. Ono, and Y. Inokuti, J. Phys. Soc. Japan 25, 88 (1968).

[9]B. W. Christ, P. M. Giles, Trans. AIME 242, 1915 (1968).

[10]P. M. Gielen and R. Kaplow, Acta Met. 15, 49 (1967).

[11]Z. Mathalone, M. Ron, J. Pipman, and S. Niedzwiedz, J. Appl. Phys. 42, 687 (1971).

[12]J. Lipkin, B. Shechter, S. Shtrikman, and D. Treves, Rev. Sci. Instr. 35, 1336 (1964).

[13]H. Shechter, M. Ron, and R. H. Herber, Nucl. Instr. Methods 44, 268 (1966).

[14]W. Kundig. Nucl. Instr. Methods 48, 219 (1967).

PHYSICAL REVIEW B VOLUME 4, NUMBER 3 1 AUGUST 1971

Infrared Absorption and Luminescence Spectra of Fe^{2+} in Cubic ZnS: Role of the Jahn-Teller Coupling

Frank S. Ham and G. A. Slack

General Electric Research and Development Center, Schenectady, New York 12301

(Received 10 March 1971)

A revised interpretation of the $^5E \rightarrow {}^5T_2$ optical absorption spectrum of Fe^{2+} in cubic ZnS is proposed. It is shown that certain absorption peaks, lacking a counterpart in the luminescence, cannot be interpreted, as previously done, as two- and three-phonon sidebands of the zero-phonon transitions, and also cannot be attributed to crystal-field electronic transitions or to simple unshifted one-phonon sidebands. A Jahn-Teller coupling within the $^5T_2$ level, weaker than the spin-orbit coupling, is shown to be capable not only of partially quenching the $^5T_2$ spin-orbit splitting but also of shifting the associated one-phonon levels in the manner required to account for the observed spectra. Such a dynamic Jahn-Teller effect, involving simultaneous coupling to a low-frequency mode (~ 100 cm^{-1}) and a higher-frequency mode (~ 300 cm^{-1}), is proposed to account for the data for Fe^{2+} in ZnS in terms of coupling to the TA and TO and/or LO phonons of the ZnS lattice. This interpretation of the phonon coupling is shown to be consistent with a moment analysis of the broadening of the optical absorption and luminescence spectra using the methods of Henry, Schnatterly, and Slichter. The relation of this model to similar features in the spectrum of Fe^{2+} in CdTe, $MgAl_2O_4$, ZnSe, ZnTe, CdS, GaP, and GaAs is discussed. It is also shown that this model provides insights into the relationship between lattice phonons and the localized modes that dominate the Jahn-Teller coupling in strongly coupled systems, and that it shows why the cluster model for the Jahn-Teller ion and its nearest neighbors often works well for such systems.

I. INTRODUCTION

The optical absorption spectrum in the near infrared of the Fe^{2+} ion in cubic ZnS, CdTe, and $MgAl_2O_4$ has been studied by Slack, Ham, and Chrenko (SHC).[1] It was found that the structure in these spectra, which correspond to the $^5E \rightarrow {}^5T_2$ transition, was not in agreement with the predictions of simple crystal-field (or ligand-field) theory for Fe^{2+} in a tetrahedral site. The dynamic Jahn-Teller effect was shown to offer a possible explanation for these discrepancies, and for ZnS: Fe^{2+} a phenomenological model involving strong Jahn-Teller coupling in the $^5T_2$ state was proposed which fit quantitatively the observed zero-phonon structure at the low-energy edge of the low-temperature absorption spectrum. According to this interpretation, the absorption peaks at higher energy arose from phonon-assisted transitions in which the emission of one, two, or three phonons of the ZnS lattice accompanied the electronic transition. Subsequently, however, Slack and O'Meara[2] observed the corresponding $^5T_2 \rightarrow {}^5E$ luminescence at liquid-helium temperature and found that the only vibronic sidebands accompanying the zero-phonon emission lines were those corresponding to the emission of *one* phonon. Since the absence of two- and three-phonon sidebands in the luminescence spectrum is inconsistent with the presence of strong peaks of this type in absorption, the previously proposed interpretation

of the absorption spectrum clearly requires revision. It is the purpose of this paper to reexamine the interpretation of these spectra in the light of recent advances[3–8] in understanding the role of the Jahn-Teller effect in modifying optical spectra.

One is tempted, of course, to try to interpret the absorption and luminescence spectra in terms of the electronic transitions expected in the crystal-field model for ZnS: Fe^{2+}, while attributing the additional peaks to simple unshifted one-phonon sidebands[9] of these transitions. This approach fails because certain phonons would then appear to be involved in the absorption spectrum which produce no corresponding phonon sideband in the luminescence. On the other hand, the Jahn-Teller interaction is capable not only of changing the spin-orbit splitting of a degenerate electronic state,[3] but also of splitting and shifting the associated higher vibronic levels.[10–14] In our revised interpretation we attribute a number of the peaks in the absorption spectrum to the effect of the Jahn-Teller coupling in displacing and mixing the vibronic states arising from the $^5T_2$ spin-orbit states through coupling with the ZnS lattice phonons. The resulting level shifts are found to be quite large, although the Jahn-Teller coupling cannot be as strong as supposed by the previous model of SHC[1] for ZnS: Fe^{2+} and, in particular, is evidently weaker than the spin-orbit interaction.

The present model is quite similar to one used by Ham, Schwarz, and O'Brien[7] to treat the effect of the Jahn-Teller coupling in reducing the spin-orbit splitting of the $^5T_2$ ground state of MgO: Fe^{2+}. In both models, the Jahn-Teller coupling is taken to be weaker than the spin-orbit interaction, and the displacement of the levels that results from the coupling is obtained by second-order perturbation theory. For MgO: Fe^{2+}, however, the interest was in the effects of the coupling on the lowest electronic spin-orbit levels of the $^5T_2$ state (the Γ_5 level with $J'=1$ and the Γ_3 and Γ_4 levels with $J'=2$; see Sec. II), and the coupling was taken to be with phonons (or a band of phonons) with frequencies in the range 300–400 cm^{-1} (where "frequencies" here are expressed in wave-number units), substantially larger than the ~200-cm^{-1} spin-orbit separation of the $J'=1$ and 2 levels expected from crystal-field theory. In the present work we are interested particularly not only in the Γ_5 ground state, but also in the higher Γ_5 vibronic levels which account for the sidebands in the optical spectrum at liquid-helium temperature and which originate in states corresponding to one excited vibrational quantum. Moreover, in the ZnS lattice we have several distinct groups of phonons in the range 70–350 cm^{-1} corresponding to critical points in the lattice frequency spectrum (see Sec. III), the separate contributions of which we wish to distinguish. We shall be particularly concerned with the effect of the Jahn-Teller coupling on the vibronic states associated with a phonon of frequency smaller than the spin-orbit splitting of the $J'=1$ and 2 levels, and with the interaction between excited states associated with different phonons. Neither of these effects was considered in the earlier work.[7]

The present work provides some new perspectives into the role of dynamic Jahn-Teller effects in modifying the optical spectra of impurity ions in crystals, while providing a detailed treatment of a microscopic model for these effects in one such system. In addition, our consideration of simultaneous Jahn-Teller coupling with several different phonons provides some useful insights into the as yet largely unresolved question of the relationship between lattice phonons and localized modes associated with a strongly coupled Jahn-Teller ion.

Our primary concern in this paper will be with the case of Fe^{2+} in cubic ZnS. We will show, however, that similar conclusions account at least qualitatively for corresponding features in the absorption spectrum of Fe^{2+} in[1,15] CdTe and[1] $MgAl_2O_4$ and in a number of other II-VI and III-V compound semiconductors.[16,17]

II. STATIC CRYSTAL-FIELD THEORY

The ground state of Fe^{2+} ($3d^6$) at a substitutional Zn site in cubic ZnS (tetrahedral site symmetry) is the orbital doublet ^5E, while the triplet $^5T_2$ is higher by the cubicfield energy Δ (equal to $10|Dq|$), determined by SHC[1] to be 3400 cm^{-1}. The spin-orbit splitting of these states[18] as given by crystal-field theory for a static lattice is shown in Fig. 1.

The separation of the five ^5E spin-orbit levels (Fig. 1) is uniform, to the accuracy of a second-order perturbation treatment of the spin-orbit coupling between ^5E and $^5T_2$, and it is given by

$$K=6[(\lambda^2/\Delta)+\rho], \tag{1}$$

where λ is the effective spin-orbit coupling parameter[1] and ρ the coefficient in the effective spin-spin interaction[19] within the states derived from the ^5D term of the free Fe^{2+} ion. Because of covalency and other effects of the crystal environment, these parameters may depart from their free-ion values λ_0 and ρ_0 given by $\lambda_0=-104.2$ cm^{-1} and $\rho_0=+1.04$ cm^{-1} and obtained from a least-squares fit to the spectroscopic data.[20] The separation K for ZnS: Fe^{2+} has been determined experimentally from far-infrared measurements[21] and magnetic susceptibility studies[22] to be $K=(+15.0\pm0.1)cm^{-1}$.

Within the $^5T_2$ state the combined effect of the spin-orbit and spin-spin interactions may be represented[1] (to second order in λ/Δ) by

$$\mathcal{H}_{so}(^5T_2)=\zeta(\vec{\mathfrak{L}}\cdot\vec{\mathfrak{S}})+\mu(\vec{\mathfrak{L}}\cdot\vec{\mathfrak{S}})^2 + \eta(\mathfrak{L}_x^2S_x^2+\mathfrak{L}_y^2S_y^2+\mathfrak{L}_z^2S_z^2), \tag{2}$$

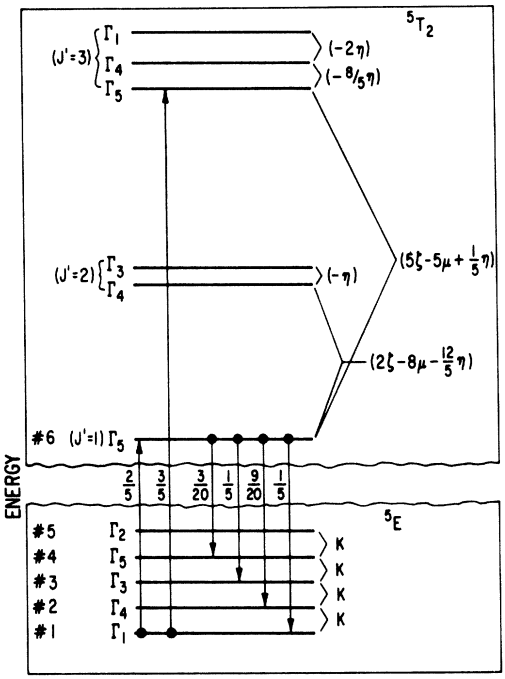

FIG. 1. Energy levels of Fe^{2+} $(3d^6)$ as predicted by crystal-field theory for tetrahedral coordination (point symmetry T_d), drawn under the assumption $\eta < 0$. Arrows indicate the two optical transitions from lowest level (Γ_1) of ^5E and the four transitions from lowest (Γ_5) level of $^5T_2$ which are electric-dipole allowed. Also shown are relative oscillator strengths predicted for individual transitions in absorption and luminescence spectra at temperatures so low that only lowest spin-orbit level of initial state is populated. [After SHC (Ref. 1), Fig. 10 and Table X.]

where $\vec{\mathcal{L}} = (\mathcal{L}_x, \mathcal{L}_y, \mathcal{L}_z)$ (x, y, z denote the cubic axes) is a vector operator defined[1] with respect to the T_2 orbital triplet states to simulate an effective orbital angular momentum with $\mathcal{L} = 1$. The crystal-field values for the parameters ζ, μ, and η are

$$\zeta = -\lambda + 2(\lambda^2/\Delta) - \tfrac{3}{2}\rho\,,$$
$$\mu = +2(\lambda^2/\Delta) - 3\rho\,, \qquad (3)$$
$$\eta = -6(\lambda^2/\Delta) + 6\rho\,.$$

The resulting separations of the spin-orbit levels of $^5T_2$ are given in Fig. 1, where the levels are labeled by the eigenvalue $J' = 1, 2, 3$ of the effective total angular momentum operator[1]

$$\vec{J} = \vec{\mathcal{L}} + \vec{S} \qquad (4)$$

to which each group of levels belongs. This characterization is accurate so long as we have $|\zeta| \gg |\eta|$.

Electric-dipole transitions[23] from the Γ_1 ground-state singlet level of ^5E are allowed in perfect tetrahedral symmetry only to levels belonging to Γ_5.

The static crystal-field model predicts two such transitions to the levels of $^5T_2$; these are indicated in Fig. 1. The relative oscillator strengths for these transitions, also given in Fig. 1 as the fraction of the oscillator strength of the full $^5E \rightarrow {}^5T_2$ absorption band associated with each transition, were calculated by SHC[1] for the static crystal-field model. Only these two transitions are expected for the crystal-field model at the lowest temperatures, at which only the Γ_1 level of ^5E is significantly populated. Selection rules and oscillator strengths for transitions originating in the higher levels of ^5E and appearing at higher temperature were also obtained by SHC (see Tables IX and X of Ref. 1).

The luminescence spectrum originating in the lowest spin-orbit level of $^5T_2$, the $\Gamma_5(J' = 1)$ level, should comprise four lines corresponding to electric-dipole-allowed transitions to the four lower levels $(\Gamma_1, \Gamma_4, \Gamma_3, \Gamma_5)$ of ^5E. The relative intensities of these lines, as predicted by the crystal-field model and obtained from Table X of SHC,[1] are given in Fig. 1 (with no account taken of possible reabsorption).

III. PHONON SPECTRUM OF CUBIC ZnS

In considering the vibronic sidebands to be expected in the optical spectra when we augment the static crystal-field model by including the electron-phonon interaction, we must know the frequencies and symmetries of the lattice phonons at the various critical points in the phonon density of states. We shall be particularly interested in those critical points which occur at the symmetry points Γ, X, and L in the Brillouin zone, where the symmetry (Table I) imposes strong selection rules on the involvement of each phonon in the optical transitions. Although peaks in the density of states of the effective phonons do not need to correspond to these symmetry points, these selection rules are useful in indicating if lattice phonons from the neighboring region of the zone are likely to contribute to a given type of coupling.

Data on the phonon spectrum of cubic ZnS have been obtained from various optical studies,[24-26] from calculations of the dispersion curves,[27-30] and very recently from neutron-inelastic-scattering experiments.[30,31] The assignment of the phonon frequencies at the principal symmetry points on the basis of the most recent data is given in Table I. The critical point of lowest frequency in the transverse acoustic (TA) branch occurs at L, with a value ~ 70 cm^{-1}. The value for TA(X) is slightly higher, ~ 90 cm^{-1}. The neutron-inelastic-scattering data[30,31] show that a maximum in the TA branch occurs near the point K at about 125 cm^{-1} and that the lower mode of the (split) TA branch is relatively flat in the region of the zone surface between X and K. The longitudinal acoustic (LA) branch is

TABLE I. Phonon frequencies and symmetries[a] for cubic ZnS.

Phonon[b]	Point Group[c] $\mathcal{G}_0(\vec{k})$	Rep.[c] of $\mathcal{G}_0(\vec{k})$ (Zn site)[d]	Rep.[c] of $\mathcal{G}_0(\vec{k})$ (S site)[d]	Rep.[e] of T_d (Zn site)	Frequency (cm^{-1})	Ref.
TO(Γ)	T_d	f	f	f	276	g
LO(Γ)	T_d	f	f	f	351	g
TA(X)	D_{2d}	Γ_5	Γ_5	$\Gamma_4+\Gamma_5$	90	h
LA(X)	D_{2d}	Γ_4	Γ_1	Γ_5	205	h
TO(X)	D_{2d}	Γ_5	Γ_5	$\Gamma_4+\Gamma_5$	305	h
LO(X)	D_{2d}	Γ_1	Γ_4	$\Gamma_1+\Gamma_3$	325	h
TA(L)	C_{3v}	Γ_3	Γ_3	$\Gamma_3+\Gamma_4+\Gamma_5$	70	h
LA(L)	C_{3v}	Γ_1	Γ_1	$\Gamma_1+\Gamma_5$	185	h
TO(L)	C_{3v}	Γ_3	Γ_3	$\Gamma_3+\Gamma_4+\Gamma_5$	295	h
LO(L)	C_{3v}	Γ_1	Γ_1	$\Gamma_1+\Gamma_5$	335	h
$TA_1(K)$	C_s	Γ_2	Γ_2	$\Gamma_2+\Gamma_3+2\Gamma_4+\Gamma_5$	90	h
$TA_2(K)$	C_s	Γ_1	Γ_1	$\Gamma_1+\Gamma_3+\Gamma_4+2\Gamma_5$	125	h
LA(K)	C_s	Γ_1	Γ_1	$\Gamma_1+\Gamma_3+\Gamma_4+2\Gamma_5$	200	h

[a]After R. Loudon, Proc. Phys. Soc. (London) 84, 379 (1964).

[b]Symmetry points in the Brillouin zone, as given by the following representative $\vec{k}$ vectors, are labeled using the notation of BSW [L. P. Bouckaert, R. Smoluchowski, and E. Wigner, Phys. Rev. 50, 58 (1936)] as in the Brillouin zone of the fcc lattice: $\Gamma(\vec{k}=0)$; $X[\vec{k}=(2\pi/a)(1,0,0)]$; $L[\vec{k}=(2\pi/a)(1/2,1/2,1/2)]$; $K[\vec{k}=(2\pi/a)(3/4,3/4,0)]$; $W[\vec{k}=(2\pi/a)(1,1/2,0)]$. Note that each point K is fully equivalent to two of the points labeled $U[\vec{k}=(2\pi/a)(-1/4,-1/4,\pm1)]$ by BSW.

[c]The notation for the point group $\mathcal{G}_0(\vec{k})$ associated with the group of the $\vec{k}$ vector and for the irreducible representations of these point groups is that of the tables of Koster, Dimmock, Wheeler, and Statz (Ref. 33).

[d]The elements of $\mathcal{G}_0(\vec{k})$ may be taken to be rotations (proper and improper) with respect to *either* a Zn site *or* a S site as origin. A function belonging to a given irreducible representation of the group of the $\vec{k}$ vector (a space group) may then at certain points in $\vec{k}$ space belong to different irreducible representations of $\mathcal{G}_0(\vec{k})$, depending on which type of site is chosen as origin for the rotations. The corresponding assignments for the different choice of origin are listed in separate columns of the table.

[e]This column lists the irreducible representations of point group T_d which are spanned by functions belonging to the given representation of $\mathcal{G}_0(\vec{k})$ at the several nonequivalent points in $\vec{k}$ space belonging to star of $\vec{k}$. Zn site is chosen as the origin for rotations in point group T_d.

[f]TO and LO branches would be degenerate at Γ ($\vec{k}=0$), and the corresponding three modes of vibration would belong as partners to irreducible representation Γ_5 of point group $\mathcal{G}_0(\vec{k}=0)=T_d$ (using either Zn or S site as origin), were it not for long-range nature of the Coulomb force produced by electric polarization induced by these vibrations in ionic lattice.

[g]Data from first-order Raman effect. O. Brafman and S. S. Mitra, Phys. Rev. 171, 931 (1968); see, also, W. G. Nilsen, *ibid.* 182, 838 (1969).

[h]Data from neutron inelastic scattering. J. Bergsma, Phys. Letters 32A, 324 (1970); see also L. A. Feldkamp, G. Venkataraman, and J. S. King, Solid State Commun. 7, 1571 (1969).

much higher than the TA branch throughout most of the zone, and it too is relatively flat in the region between X, K, and L. These features lead us to expect two peaks in the phonon density of states from the acoustic branch, one with a broad maximum in the energy range of the two TA modes at K, the other a narrower peak near the maximum in the LA branch. The optical branches are separated from the LA branch by a gap. The most recent neutron data[30] show that both the TO and LO branches are fairly narrow and that they are separated by a small gap. The TO branch has its minimum at 276 cm^{-1} at Γ and its maximum at ~ 305 cm^{-1} at X, and it should thus contribute a strong peak to the density of states within this range. The LO branch conversely has its minimum at ~ 325 cm^{-1} at X and its maximum at 351 cm^{-1} at Γ, and thus contributes a smaller peak in this range.

In addition to the frequencies, Table I also shows the symmetry classification of the phonons in terms of the irreducible representation of the point group associated with the group of the $\vec{k}$ vector to which the phonon belongs.[32] It must be noted that in the zinc-blende structure the operations comprising these point groups may be defined with respect to either the Zn site or S site as origin, and that at the point X the representation of the point group to which a given phonon belongs is different depending on which choice is made. Associated with this symmetry difference, it may be shown that a LA or LO mode at X involves *either* motion of the Zn ions *or* that of the S ions. Since the Zn mass is larger than the S mass, while the force constants involved in each mode should be similar, we assume that the LA(X) mode involves the motion of the Zn and the LO(X) mode the S. The phonon symmetries[33] are then determined as given in Table I.

From the lattice phonons of a given type corresponding to the several inequivalent $\vec{k}$ vectors in the star of $\vec{k}$, it is possible to form linear combinations belonging to the various irreducible representations of the point group of any site in the crystal. The

representations of the point group T_d of a Zn site (which are different at X from those appropriate to a S site), to which the possible combinations of each type of phonon belong, are also listed in Table I. These results determine the selection rules for the participation of the lattice phonons in the various types of electron-phonon interaction with an impurity ion on a Zn site to be discussed in Sec. IV.

IV. JAHN-TELLER EFFECTS

The interaction between the lattice vibrations of the crystal and the electrons of an Fe^{2+} ion at a substitutional Zn site may be expressed in the form

$$\mathcal{H}_{ep}=\sum_{p,i} V_p(i)\sum_q U_q^p(i)Q_q^p(i) \tag{5}$$

to first order in the distortion modes $Q_q^p(i)$. Here the $Q_q^p(i)$ are taken to be independent real linear combinations of the ion displacements chosen to transform by the qth row of the irreducible representation Γ_p of the point group T_d of the Fe^{2+} site. The $U_q^p(i)$ are real Hermitian electronic operators having the same transformation behavior as the $Q_q^p(i)$, and the $V_p(i)$ are real coefficients. $\mathcal{H}_{ep}$ as given by Eq. (5) is then invariant under T_d. We assume that in the harmonic approximation to the lattice vibrations of the crystal containing the Fe^{2+} the $Q_q^p(i)$ would represent normal modes of vibration if the electron-phonon interaction with the Fe^{2+} as given by Eq. (5) were ignored. The terms in the Hamiltonian representing the elastic and kinetic energies of the lattice vibrations are thus given by

$$\mathcal{H}_{lat}=\sum_{p,i}\tfrac{1}{2}[\mu_p(i)]^{-1}\sum_q\{[P_q^p(i)]^2+[\mu_p(i)\omega_p(i)]^2[Q_q^p(i)]^2\}\ , \tag{6}$$

where $P_q^p(i)$ is the momentum conjugate to $Q_q^p(i)$ and $\mu_p(i)$ and $\omega_p(i)$ are, respectively, the effective mass and angular frequency of the ith mode belonging to Γ_p (which thus has a degeneracy given by the dimension of Γ_p). Some of these modes may be localized modes associated with the Fe^{2+} impurity, whereas others represent modes within the phonon bands of the host crystal, as perturbed by the impurity's presence.

Many of the terms in Eq. (5) provide coupling between different electronic levels of the Fe^{2+}. The only terms[34] that contribute to the Jahn-Teller coupling of an orbital triplet $T_2(\Gamma_5)$ state, that is, to a direct splitting of the triplet linear in Q, are the distortion modes[35] belonging to Γ_3 and Γ_5. We may rewrite these terms in Eq. (5) which express the Jahn-Teller coupling of the $^5T_2$ state of the Fe^{2+} ion to a doubly degenerate mode Q_θ, Q_ϵ belonging to Γ_3 and a triply degenerate mode Q_ξ, Q_η, Q_ζ belonging to Γ_5 in the following standard form[7]:

$$\mathcal{H}_{JT}(^5T_2)=V_E(Q_\theta\mathcal{E}_\theta+Q_\epsilon\mathcal{E}_\epsilon)$$
$$+V_T(Q_\xi\mathcal{T}_\xi+Q_\eta\mathcal{T}_\eta+Q_\zeta\mathcal{T}_\zeta)\ . \tag{7}$$

The electronic operators are defined in terms of $\mathfrak{L}_x$, $\mathfrak{L}_y$, and $\mathfrak{L}_z$ as follows[7]:

$$\mathcal{E}_\theta=\mathfrak{L}_z^2-\tfrac{1}{2}(\mathfrak{L}_x^2+\mathfrak{L}_y^2)=\tfrac{3}{2}\mathfrak{L}_z^2-\mathfrak{I}\ ,$$
$$\mathcal{E}_\epsilon=\tfrac{1}{2}\sqrt{3}(\mathfrak{L}_x^2-\mathfrak{L}_y^2)\ ,$$
$$\mathcal{T}_\xi=(\mathfrak{L}_y\mathfrak{L}_z+\mathfrak{L}_z\mathfrak{L}_y)\ , \tag{8}$$
$$\mathcal{T}_\eta=(\mathfrak{L}_z\mathfrak{L}_x+\mathfrak{L}_x\mathfrak{L}_z)\ ,$$
$$\mathcal{T}_\zeta=(\mathfrak{L}_x\mathfrak{L}_y+\mathfrak{L}_y\mathfrak{L}_x)\ ,$$

and $\mathfrak{I}$ denotes the unit matrix.

One frequently assumes in treating a Jahn-Teller problem that it suffices to assume coupling with a single normal mode of each allowed symmetry type, as in Eq. (7), either because these modes are true local modes which dominate the electron-phonon coupling with the defect, or because one approximates the effect of coupling to many lattice modes by a single effective mode of some average frequency. A justification for this latter approximation in treating the effect of Jahn-Teller coupling to many lattice modes on the spin-orbit splitting and other properties of the lowest electronic levels of the $^5T_{2g}$ state of the Fe^{2+} ion in MgO has been given by Ham, Schwarz, and O'Brien.[7] In the present case, however, we are interested in considering all of the vibronic sidebands of the $^5E\rightarrow{}^5T_2$ optical transition, and the data[1,2] indicate that more than one mode of each type may be important. We want to try to relate such modes to the modes of the ZnS lattice considered in Sec. III, in particular to those critical points in the phonon spectrum which contain modes of symmetry Γ_3 or Γ_5 with respect to the Zn site, as indicated in the fifth column of Table I. In general, then, we may expect the Jahn-Teller coupling for the $^5T_2$ state of the Fe^{2+} to be given by several different terms of each type in Eq. (7), representing lattice modes of different frequency of each of the two symmetry types.

It had been shown[3] prior to the work of SHC[1] that the Jahn-Teller coupling may cause a partial quenching of the spin-orbit interaction. On this basis, and making the basic assumption that the Jahn-Teller coupling is strong compared with the spin-orbit interaction, SHC sought to explain the zero-phonon structure in the absorption spectrum. With the Hamiltonian for a dynamic Jahn-Teller effect in an orbital triplet state given by combining the appropriate terms of the form of those in Eq. (7) with the corresponding terms from Eq. (6), one finds that the lowest vibronic level of this Hamiltonian remains triply degenerate. These degenerate vibronic states are different mixtures of vibrational

wave functions from different levels of the unperturbed harmonic-oscillator Hamiltonian (6), and matrix elements of the spin-orbit interaction between these degenerate states are consequently reduced from their crystal-field values. A Hamiltonian of the form in Eq. (2) may, nevertheless, still suffice to describe the spin-orbit splitting of this level, but the coefficients ζ, μ, and η may now have values very different from those given by crystal-field theory in Eq. (3). A set of values for these coefficients in a phenomenological Hamiltonian of this form was obtained by SHC[1] which fit the observed zero-phonon structure at the low-energy edge of the absorption spectrum.

A further important consequence of the Jahn-Teller coupling in the $^5T_2$ state in producing vibronic states which mix vibrational wave functions from different levels of the unperturbed lattice oscillators is that optical transitions from the ^5E ground state to excited vibronic levels of $^5T_2$ become allowed. This is one of several ways in which intensity is transferred by the electron-phonon coupling from the allowed electronic transitions considered in Sec. II to the vibronic sidebands.[9] If we assume (as discussed below) that Jahn-Teller effects in the ^5E state may be ignored, then the initial state for optical transitions at temperatures close to 0 °K is the Born-Oppenheimer vibronic state in which the electronic wave function is that of the Γ_1 spin-orbit level of ^5E (Fig. 1) and the vibrational state of the lattice is that in which all of the oscillators of $\mathcal{H}_{\text{lat}}$ in Eq. (6) are in their $n=0$ ground state. The optical transition probability to one of the vibronic states of $^5T_2$ is then obtained from the product of the appropriate electronic transition probabilities with the fraction of the unperturbed $n=0$ state of each oscillator which is admixed in the final state. We may obtain the resulting distribution of oscillator strength very simply under the assumptions appropriate to the model proposed by SHC[1] if we further assume that the Jahn-Teller coupling is with a single Γ_3 mode. The Jahn-Teller coupling does not mix the electronic states of the orbital triplet in this case, and the associated vibrational states are simply those of the simple harmonic oscillator displaced to one of the three positions in Q_θ, Q_ϵ space at which the electronic energy (including the elastic energy of the statically distorted lattice) has a minimum. From the overlap integrals[3] between the states of the displaced oscillator and the $n=0$ state of the unperturbed oscillator, one can show very easily that the relative probability of an optical transition to the nth vibronic level of $^5T_2$ (that is, a transition in which we can say that n vibrational quanta have been excited) is given by a Poisson distribution

$$p_n = (n!)^{-1}(S_E)^n e^{-S_E} . \tag{9}$$

Here the Huang-Rhys parameter[36] S_E is given by the ratio of the Jahn-Teller energy of the $^5T_2$ state for this case

$$(E_{JT})_E = V_E^2/2\mu_E\omega_E^2 \tag{10}$$

to the phonon energy

$$S_E = (E_{JT})_E/\hbar\omega_E . \tag{11}$$

Conversely, Eq. (9) also gives the relative probability in the same case for the excitation of n vibrational quanta in the reverse luminescent transition from the lowest vibronic level of the Jahn-Teller distorted $^5T_2$ state to the undistorted ^5E state.

We find, therefore, that the presence of sidebands in the $^5E \rightarrow {}^5T_2$ absorption spectrum corresponding to the simultaneous emission of two and three lattice phonons leads us to expect corresponding two- and three-phonon sidebands of similar relative intensity in the $^5T_2 \rightarrow {}^5E$ luminescence spectrum. Although the simple distribution given by Eq. (9) will not hold in detail for a case of more complicated Jahn-Teller coupling than with a single Γ_3 mode, this qualitative conclusion concerning the reciprocal relationship between the relative intensities of the vibronic sidebands in the absorption and luminescence spectra will be generally true.[37] In the model proposed by SHC for ZnS: Fe^{2+} many of the strong peaks in the $^5E \rightarrow {}^5T_2$ absorption spectrum were identified with phonon-assisted transitions involving the emission of two or three phonons. The absence of sidebands involving the excitation of more than one phonon in the $^5T_2 \rightarrow {}^5E$ luminescence spectrum[2] (see Sec. V) shows therefore that the basic assumption of the SHC model that the Jahn-Teller coupling is stronger than the spin-orbit interaction cannot be correct for ZnS: Fe^{2+}.

When the Jahn-Teller coupling is *not* strong with respect to the spin-orbit coupling, one can no longer proceed by first solving the Jahn-Teller problem for the orbital states and subsequently considering the spin-orbit splitting of these vibronic levels. Accordingly, in considering a Jahn-Teller coupling weaker than or possibly comparable with the spin-orbit splitting of the $^5T_2$ state, we follow the method of Ham, Schwarz, and O'Brien[7] and treat the Jahn-Teller coupling by second-order perturbation theory. We have considered in the Appendix the special case in which this coupling is with two Γ_3 modes,[38] and we have obtained there the Jahn-Teller displacements of a number of the zero- and one-phonon vibronic levels of the Fe^{2+}, together with the resulting intensities of the corresponding one-phonon sidebands in the optical absorption and emission spectra. We must emphasize, however, that because second-order perturbation theory becomes increasingly inaccurate for the higher vibronic levels as a means of treating the Jahn-Teller cou-

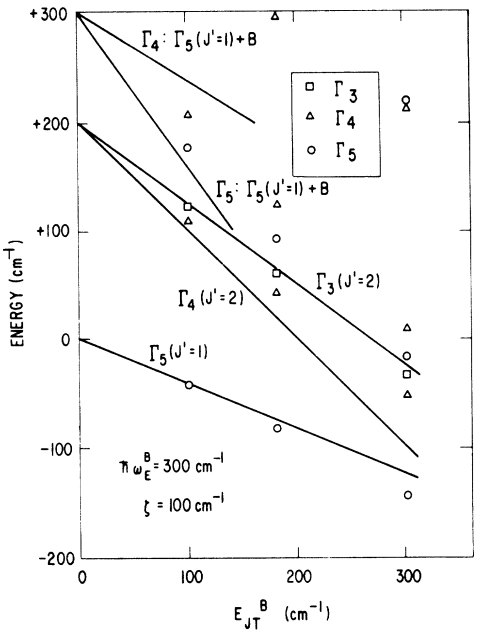

FIG. 2. Spin-orbit energy levels Γ_5 ($J'=1$) and Γ_3, Γ_4 ($J'=2$) of $^5T_2$ term of Fe^{2+} ion in tetrahedral symmetry, as a function of Jahn-Teller energy E_{JT}^B [Eq. (10) of text] for coupling with one doubly degenerate Γ_3 vibrational mode (B) with $\hbar\omega_E^B = 300$ cm^{-1}. Also shown are the one-phonon levels Γ_4 and Γ_5 derived from Γ_5 ($J'=1$) with excitation of one B phonon. Straight lines show results of treating the Jahn-Teller interaction by second-order perturbation theory, and the points were obtained by direct numerical diagonalization of energy matrix by Ham, Schwarz, and O'Brien (Ref. 7). (Also shown in the upper right-hand corner are numerically calculated energies of two higher levels.) Spin-orbit parameter ζ from Fig. 1 is taken to be $\zeta = +100$ cm^{-1}, and second-order spin-orbit splitting is neglected ($\mu = \eta = 0$).

pling between the different $^5T_2$ spin-orbit levels of the Fe^{2+}, our perturbation results are not quantitatively accurate once the Jahn-Teller coupling is moderately strong. Nevertheless, our results for this special case provide a basis for a qualitative understanding of the role of the Jahn-Teller coupling in the even more complicated situation appropriate to the Fe^{2+} ion in an actual crystal.

We show in Fig. 2, from the results of the Appendix and from the work of Ham, Schwarz, and O'Brien,[7] the energies of the Γ_5 ($J'=1$) and Γ_3, Γ_4 ($J'=2$) levels of the $^5T_2$ term of the Fe^{2+} (see Fig. 1, where we have taken $\zeta = +100$ cm^{-1} and have set $\mu = \eta = 0$ for simplicity) as a function of the Jahn-Teller energy E_{JT}^B [Eq. (10)], when the coupling is with one Γ_3 mode (B) with $\hbar\omega_E^B = 300$ cm^{-1}. Also shown are the displacements of the lowest one-phonon levels, Γ_4 and Γ_5, which derive, in the limit $E_{JT}^B = 0$, from the Γ_5 ($J'=1$) electronic state with the excitation of one B phonon. The straight lines in Fig. 2 show the second-order perturbation results, while the points show the results of the more accurate numerical calculations of Ham, Schwarz, and O'Brien.[7,39] We see not only that the spin-orbit splitting between the zero-phonon $J'=1$ and 2 levels is reduced by the Jahn-Teller coupling[3,7] but also that the one-phonon Γ_4, Γ_5 levels are depressed relative to the $J'=1$ ground state by this coupling. If the excitation energy of these latter levels is taken to give the frequency of an effective vibrational mode of the coupled electron-phonon system, we see then that this frequency is reduced by the Jahn-Teller coupling.

Figure 2 shows the effect of the Jahn-Teller coupling with a phonon for which $\hbar\omega_E^B$ is larger than the spin-orbit splitting 2ζ of the $J'=1$ and 2 electronic states, whereas Fig. 3 shows the corresponding results for coupling to a single Γ_3 mode (A) having $\hbar\omega_E^A < 2\zeta$, namely, $\hbar\omega_E^A = 100$ cm^{-1}. In Fig. 3, we have plotted the energies of the levels relative to that of Γ_5 ($J'=1$), so that (in contrast to Fig. 2) we can see directly from the slope of each line the extent to which the Jahn-Teller coupling reduces the excitation energy of the level above the ground state. We have also included not only the Γ_4, Γ_5 one-phonon levels derived from Γ_5 ($J'=1$) but also

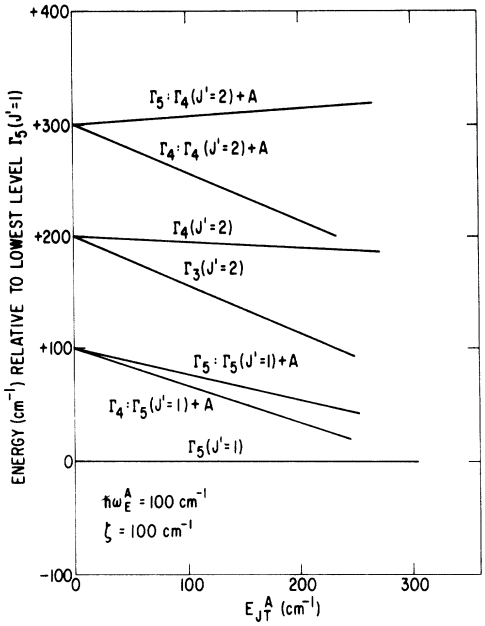

FIG. 3. Relative energies of spin-orbit levels Γ_5 ($J'=1$) and Γ_3, Γ_4, ($J'=2$) of the $^5T_2$ term of Fe^{2+} (T_d symmetry), and of one-phonon levels Γ_4 and Γ_5 derived from Γ_5 ($J'=1$) and Γ_4 ($J'=2$) with excitation of one A phonon, as a function of the Jahn-Teller energy E_{JT}^A, for coupling to one Γ_3 mode (A) with $\hbar\omega_E^A = 100$ cm^{-1}. Straight lines show energies relative to that of Γ_5 ($J'=1$) to the accuracy of treating the Jahn-Teller coupling by second-order perturbation theory for spin-orbit parameters $\zeta = +100$ cm^{-1}, $\mu = \eta = 0$.

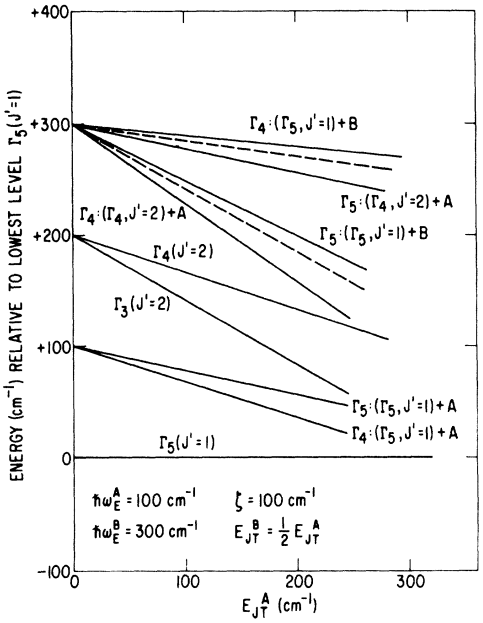

FIG. 4. Relative energies of spin-orbit levels Γ_5 ($J'=1$) and Γ_3, Γ_4 ($J'=2$) of the $^5T_2$ term of Fe^{2+} (T_d symmetry), and of one-phonon levels Γ_4 and Γ_5 derived from Γ_5 ($J'=1$) and Γ_4 ($J'=2$) with excitation of either one A or one B phonon, for simultaneous Jahn-Teller coupling to two Γ_3 modes (A and E) with $\hbar\omega_E^A = 100$ cm^{-1}, $\hbar\omega_E^B = 300$ cm^{-1}. Relative coupling strengths for the two modes are arbitrarily taken such that $E_{JT}^B = \frac{1}{2}E_{JT}^A$, whereas abscissa in the figure is taken to be E_{JT}^A to facilitate comparison with Fig. 3. Solid lines show energies relative to that of Γ_5 ($J'=1$) to the accuracy of treating Jahn-Teller coupling by second-order perturbation theory but neglecting second-order coupling between nearly degenerate one-phonon states having same symmetry but involving different types of phonons (*A or B*). Dashed lines give the corrected energies of one-phonon Γ_5 levels when this second-order coupling between them is included. Spin-orbit parameters are $\zeta = +100$ cm^{-1}, $\mu = \eta = 0$.

the Γ_4, Γ_5 levels derived from Γ_4 ($J'=2$) by the excitation of one A quantum.[40]

It is shown in the Appendix that when $\hbar\omega_E^A$ is small compared with 2ζ there is a possibility that the vibronic levels derived from Γ_5 ($J'=1$) by the excitation of one to several A quanta will form a sequence simulating the levels of a simple oscillator having an effective frequency very much reduced below ω_E^A by the Jahn-Teller coupling to the excited spin-orbit levels [see Eqs. (A9) and (A10) of Appendix]. The states of this sequence are coupled only weakly with each other by the Jahn-Teller coupling [since the coefficient of the linear coupling term in Eq. (A8) is only $\frac{1}{10}$ that of the coupling of the *orbital* triplet in Eq. (A2)]. Nevertheless, if this effective frequency is sufficiently small (namely, if $E_{JT}^A \sim 2\zeta$), this coupling will still serve to mix the vibrational parts of these states appreciably and thereby cause a transfer of some of the oscillator strength of the optical absorption spectrum from the Γ_5 ($J'=1$) ground state of the sequence to the excited Γ_5 states. As we will see in Sec. V, there may be evidence of the appearance of sidebands corresponding to such an effective low-frequency mode in the absorption spectrum of Fe^{2+} in ZnS, and more prominently in CdTe.

Finally, Fig. 4 shows the effect of simultaneous Jahn-Teller coupling with both the A and B Γ_3 modes treated separately in Figs. 2 and 3. Here we have again plotted the energies relative to that of the ground state, and we have included all the one-phonon states shown previously in Figs. 2 and 3; the solid lines in Fig. 4 show the energies of each of these states to the accuracy of treating the Jahn-Teller interaction by second-order perturbation theory but ignoring any corresponding second-order coupling between different states (see below). We have arbitrarily taken $E_{JT}^B = \frac{1}{2}E_{JT}^A$ in Fig. 4, but we have plotted the levels against E_{JT}^A as the abscissa. Comparison of Figs. 3 and 4 then shows immediately the effect on each level of Fig. 3 of the additional coupling with the B mode. We see that whereas the excitation energy of the one-phonon A levels derived from Γ_5 ($J'=1$) is unaffected by the additional coupling (to our present accuracy), the Γ_3, Γ_4 ($J'=2$) levels are depressed further by a large amount, and as a consequence the same is true for the higher one-phonon A levels derived from these. The absolute displacements of all levels, of course, depend on the coupling to *all* Jahn-Teller-active modes.

As we have shown in the Appendix, the Jahn-Teller interaction leads to a second-order coupling between vibronic states which arise via the excitation of different types of phonons but which have the same over-all symmetry. We have exhibited the effect of such a coupling in Fig. 4 between the Γ_5 state which derives from Γ_5 ($J'=1$) by the excitation of one B quantum and the Γ_5 state which derives from Γ_4 ($J'=2$) via one A quantum. Since these states are degenerate for $E_{JT}^A = E_{JT}^B = 0$ for our choice of parameters (i.e., $\hbar\omega_E^A + 2\zeta = \hbar\omega_E^B$), this coupling, which is proportional to $(E_{JT}^A E_{JT}^B)^{1/2}$, simply changes the slopes of the corresponding lines in Fig. 4 [in accordance with Eq. (A12)]. The resulting energies for these two Γ_5 levels, which now represent linear combinations of the states involving the two types of excitation, are shown by the dashed lines in Fig. 4.

Although the distribution of vibronic levels for simultaneous coupling to both A and B modes is quite complex for intermediate values of E_{JT}^A and E_{JT}^B, it is of interest to note that this distribution simplifies again, once either E_{JT}^A or E_{JT}^B (or both) become large compared to 5ζ. We then have the situation which was assumed by SHC,[1] and we may

first solve the Jahn-Teller problem for the orbital states and then consider the spin-orbit splitting of the resulting levels. However, since the dynamic Jahn-Teller problem for an orbital Γ_5 triplet coupled to any number of Γ_3 modes has an immediate and simple solution[3] in which all the vibronic levels are shifted by the same amount, the relative energies of these orbital levels are just the same as in the absence of the Jahn-Teller coupling. The ground state thus remains a Γ_5 orbital state; taking account of the spin-orbit splitting (now assumed largely quenched by the strong Jahn-Teller coupling) we have that this state comprises (for $S=2$) a group of six spin-orbit levels with symmetry

$$\Gamma_5 \times (\Gamma_3 + \Gamma_5) = \Gamma_1 + \Gamma_3 + 2\Gamma_4 + 2\Gamma_5 .$$

Excited levels fall into groups higher than this lowest group by an integral multiple of the appropriate phonon frequency (or sum thereof). This grouping of the spin-orbit levels, including the appearance of the first set of excited levels roughly $\hbar\omega$ above the ground state, is already evident from the calculated points at the right-hand side in Fig. 2.[41] The arrangement of the spin-orbit levels in this lowest group may then be obtained from the theory of the dynamic Jahn-Teller effect as given by Ham,[3] and in the strong-coupling limit we obtain the distribution of spin levels which would characterize a static Jahn-Teller distortion.[42]

The fraction of the total integrated intensity of the ${}^5E \rightarrow {}^5T_2$ optical absorption spectrum at 0 °K which is transferred by the Jahn-Teller coupling to the one-phonon sidebands, or in other words, the relative probability of an optical transition (electric-dipole) from the Γ_1 level of ${}^5E$ to the various Γ_5 levels of ${}^5T_2$ that represent the excitation of one phonon, is given in Table II for the weak-coupling situation appropriate to Figs. 2–4 and the same two Γ_3 modes A and B used previously. These values are obtained [Eq. (A13)] from the first-order perturbation admixture of the zero-phonon states into the one-phonon states, on the assumption that Jahn-Teller coupling in the ${}^5E$ state is negligibly small. Also given in Table II are the corresponding relative probabilities [Eq. (A14)] for the transitions with one-phonon excitation in the ${}^5T_2 \rightarrow {}^5E$ luminescence spectrum, for which the initial state is taken to be the Γ_5 ($J'=1$) zero-phonon ground state of ${}^5T_2$. We have also included in Table II for comparison the results one obtained for the luminescence sidebands when the Jahn-Teller–active mode has Γ_5 symmetry rather than Γ_3. The distribution of sideband intensity among the individual transitions is different in the two cases and thus might offer a means for distinguishing them.

We have assumed throughout our discussion that Jahn-Teller coupling within the ${}^5E$ state is sufficiently weak to be neglected. Far-infrared studies[21] of Fe^{2+} in ZnS have indeed found no compelling evidence that Jahn-Teller effects in the ${}^5E$ state are significant; nevertheless, we cannot yet entirely rule out this possibility. If such coupling were with a low-frequency mode ($\hbar\omega \lesssim 4K$), then as shown by Vallin[43] there might be a substantial distortion of the uniform spacing of the ${}^5E$ spin-orbit levels predicted by crystal-field theory (Sec. II) and shown in Fig. 1, together with the appearance of extra lines in the far-infrared absorption spectrum. Such effects have indeed been found[15,43] for Fe^{2+} in CdTe. For Fe^{2+} in ZnS, however, the far-infrared data[21] on the splitting and relative intensities of the various optical transitions in magnetic fields up to 140 kG are described quite well by the crystal-field model.[44]

If Jahn-Teller coupling in the ${}^5E$ state were with a mode having $\hbar\omega$ greater than the spin-orbit splitting $4K$, we would have a situation similar to that treated by Ham[45] for the effect of Jahn-Teller coupling on paramagnetic resonance in a ${}^2E$ state. In particular, the spin-orbit and spin-spin interactions within ${}^5E$ that lead to the splitting shown in Fig. 1 can be shown[43] to have a form analogous to that of the anistropic part of the Zeeman interaction, so that the effect of both on the vibronic ground state is reduced by the same reduction factor q.[45] In terms of the Jahn-Teller energy $E_{JT}({}^5E)$ for the ${}^5E$ state, q may be approximated roughly by the expression[45]

$$q \simeq \tfrac{1}{2}\{1 + \exp[-4E_{JT}({}^5E)/\hbar\omega]\} . \tag{12}$$

The spin-orbit splitting of the ${}^5E$ vibronic ground state therefore remains uniform and is given in terms of the crystal-field parameters in Eq. (1) by

$$K' = qK = 6q[(\lambda^2/\Delta) + \rho] . \tag{13}$$

The main effect of a dynamic Jahn-Teller effect on the ${}^5E$ ground state is therefore to reduce the interval K between the split spin-orbit levels by possibly as much as ~ 50%. Such a reduction is difficult to distinguish in the experimental data, however, from that resulting from reductions in λ and ρ as a consequence of covalency. If, for example, we took the free-ion values for λ and ρ (Sec. II), we would obtain $K = 25.4\ \text{cm}^{-1}$, so that from the observed value[21,22] $K' = 15.0\ \text{cm}^{-1}$ we would infer from Eq. (13) $q = 0.6$, corresponding to $E_{JT}({}^5E) \simeq \tfrac{1}{2}\hbar\omega$. Alternatively, assuming $q=1$, $\rho = 1.04\ \text{cm}^{-1}$, $\Delta = 3400\ \text{cm}^{-1}$, we would infer from the observed value of K' the value $|\lambda| = 70\ \text{cm}^{-1}$.

Jahn-Teller coupling in the ${}^5E$ state provides an independent mechanism leading to vibronic sidebands in the optical absorption and luminescense spectra and interfering with the sideband intensities that we have predicted on the basis of Γ_3 mode coupling in ${}^5T_2$. Since two-phonon sidebands do not ap-

TABLE II. Fractional intensities transferred by Jahn-Teller coupling[a] in the $^5T_2$ state to one-phonon sidebands in optical absorption and emission spectra at 0 °K, as calculated from the first-order perturbation mixing of the vibronic states when the Jahn-Teller coupling is weak compared to the spin-orbit interaction.

$^5E \rightarrow {}^5T_2$ absorption spectrum; initial state: Γ_1 of ^5E

Final one-phonon state[b] of $^5T_2$	Phonon $p=A$ (Γ_3; $\hbar\omega_E^A = 100$ cm^{-1})	$p=B$ (Γ_3; $\hbar\omega_E^B = 300$ cm^{-1})
Γ_5: (Γ_5, $J'=1$) $+p$	$0.0062x_E^A$	$0.6250x_E^B$
Γ_5: (Γ_4, $J'=2$) $+p$	$0.0417x_E^A$	...

$^5T_2 \rightarrow {}^5E$ emission spectrum; initial state: Γ_5 ($J'=1$) of $^5T_2$

Final one-phonon state[c] of ^5E	Phonon $p=A$ (Γ_3; 100 cm^{-1})	$p=B$ (Γ_3; 300 cm^{-1})	$p=C$ (Γ_5; 100 cm^{-1})	$p=D$ (Γ_5; 300 cm^{-1})
(Γ_1, ^5E) $+p$	$0.0125x_E^A$	$0.0383x_E^B$	$0.000x_T^C$	$0.0031x_T^D$
(Γ_4, ^5E) $+p$	$0.0167x_E^A$	$0.0754x_E^B$	$0.0139x_T^C$	$0.0382x_T^D$
(Γ_3, ^5E) $+p$	$0.0139x_E^A$	$0.0408x_E^B$	$0.0074x_T^C$	$0.0335x_T^D$
(Γ_5, ^5E) $+p$	$0.0056x_E^A$	$0.0251x_E^B$	$0.0213x_T^C$	$0.0769x_T^D$
(Γ_2, ^5E) $+p$	$0.0014x_E^A$	$0.0025x_E^B$	$0.0074x_T^C$	$0.0304x_T^D$
Sum	$0.0500x_E^A$	$0.1821x_E^B$	$0.0500x_T^C$	$0.1821x_T^D$

[a] Corresponding parameters x_E and x_T [Ref. 7, Eq. (3.3)] used in table to give the strength of Jahn-Teller coupling are defined as follows in terms of coupling coefficients [Eq. (7)] for each type of mode:

$$x_E = (E_{JT})_E/\hbar\omega_E = V_E^2/2\hbar\mu_E\omega_E^3 \text{ for a } \Gamma_3 \text{ mode,}$$

$$x_T = 3/2(E_{JT})_T/\hbar\omega_T = V_T^2/\hbar\mu_T\omega_T^3 \text{ for a } \Gamma_5 \text{ mode.}$$

[b] Notation used to identify these states is same as that used in Figs. 2–4. Mixing of different one-phonon states through Jahn-Teller coupling in second order has not been taken into account in evaluating sideband intensities.

[c] Notation indicates final electronic state of ^5E to which transition occurs accompanied by excitation of one phonon. Since we have assumed negligible Jahn-Teller coupling within ^5E state, we do not have any splitting of the several vibronic states arising from a given electronic state via excitation of one phonon (for example, Γ_4 level of ^5E gives rise to $\Gamma_4 \times \Gamma_3 = \Gamma_4 + \Gamma_5$ vibronic states via the excitation of one Γ_3 phonon, but these remain degenerate in our model). Electric-dipole transitions from Γ_5 ($J'=1$) level are, in principle, allowed to all vibronic levels belonging to Γ_1, Γ_3, Γ_4, and Γ_5.

pear in the $^5T_2 \rightarrow {}^5E$ luminescence (Sec. V), we *can* conclude that the Jahn-Teller coupling in ^5E must not be so strong as to cause the appearance of such transitions. In the subsequent discussion in this paper we will assume for simplicity that this coupling is negligible, but we must keep in mind that this may not be so and that the reduction in K from its value obtained for free-ion parameters may be due to the combined effect of covalency and a weak Jahn-Teller coupling within ^5E.

V. EVIDENCE FOR JAHN-TELLER EFFECTS IN EXPERIMENTAL SPECTRA OF Fe^{2+} IN ZnS

Experience in understanding the role of dynamic Jahn-Teller effects in modifying the properties of transition-metal ions in crystals has accumulated[5–8, 46] rapidly since SHC[1] first suggested that these effects were important in the optical spectra of Fe^{2+} in ZnS, CdTe, and $MgAl_2O_4$. We are now able to propose the outlines of a microscopic model for Jahn-Teller effects in these systems. Nevertheless, a detailed quantitative interpretation remains out of the question at this time because of the complexity of the problem and the uncertainty in identifying individual lines and in knowing which of the many possible vibrational modes participate significantly in the coupling.

We show in Fig. 5 the optical absorption spectrum of Fe^{2+} in ZnS at 2.7 and 4.4 °K, as found by SHC,[1] and in Fig. 6 the luminescence spectrum at 5 °K obtained by Slack and O'Meara.[2] Table III lists the energies of the peaks in these low-temperature spectra and gives their position relative to that of the main zero-phonon line (1–6), which represents the transition from the Γ_1 level of ^5E to the lowest vibronic level of $^5T_2$, namely, according to our present interpretation the Γ_5 ($J'=1$) level of Fig. 1.

Comparing these absorption and luminescence spectra, we reach two immediate conclusions. First, aside from the zero-phonon lines (6-2), (6-3), and (6-4) expected from Fig. 1, the only sidebands seen in the luminescence spectrum (Fig. 6) are those corresponding to the emission of one phonon. There is one group of such peaks in the range ~70–150 cm^{-1} from the position of the zero-phonon line (1-6) (which is not seen in the low-temperature luminescence because of reabsorption),

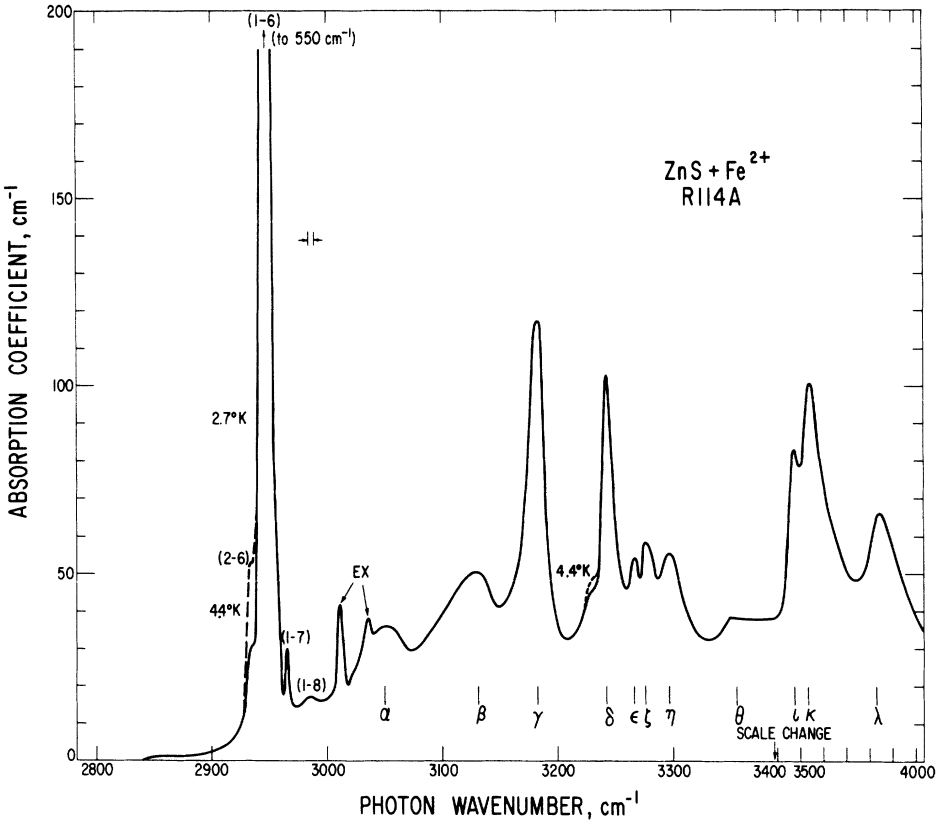

FIG. 5. Optical absorption spectrum of Fe^{2+} in cubic ZnS at 2.7 and 4.4°K [from SHC, Ref. 1, Fig. 3]. The notation used to designate some of the peaks has been changed from that of SHC, as shown in Table III. Peaks labeled *EX* are absent in other crystals and do not belong to Fe^{2+} spectrum.

and from Table I we see that these appear to correspond to the emission of a TA phonon from the vicinity of the points *X*, *L*, or *K*. A second group, in the range 300–380 cm^{-1} from (1-6), apparently corresponds to the emission of one TO or LO phonon. No peaks corresponding to the emission of two TA, TO, or LO phonons are evident. From our discussion of the intensity distribution in vibronic sidebands in connection with Eq. (9) of Sec. IV [a similar distribution would be obtained also for cou-

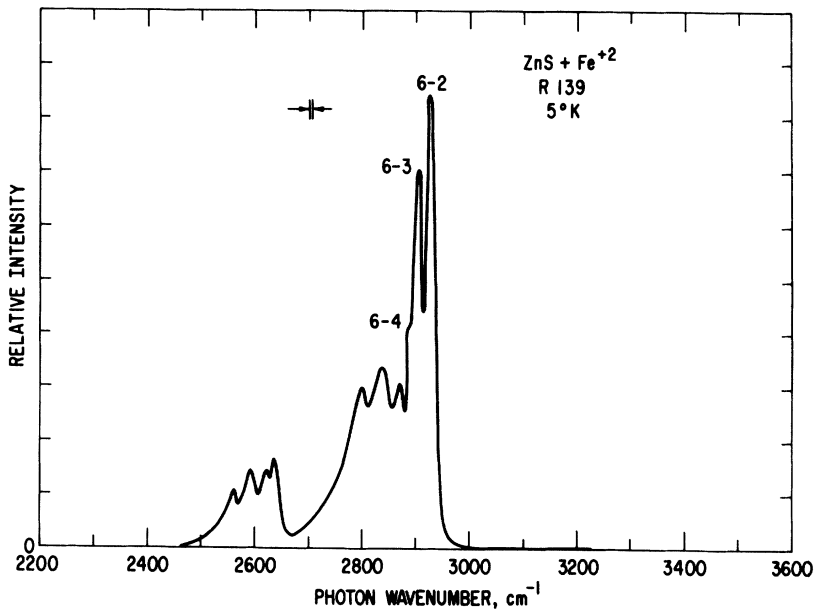

FIG. 6. Relative intensity of luminescence spectrum of Fe^{2+} in cubic ZnS at 5°K. Mole fraction of FeS in ZnS: 1.0×10^{-4} [from Slack and O'Meara, Ref. 2, Fig. 1(b)].

TABLE III. Absolute and relative energies of various peaks in the optical absorption and luminescence spectra of Fe^{2+} in cubic ZnS. [a]

Peak energy (absolute) (cm^{-1})	Designation for peak		Peak energy[b] [relative to line (1-6)] (cm^{-1})
	Present work	Refs. 1 and 2	
Absorption spectrum			
2899	(4-6)	(4-6)	−46[c]
2919	(3-6)	(3-6)	−26[c]
2930	(2-6)	(2-6)	−15[c]
2945	(1-6)	(1-6)	0[c]
2964	(1-7)	(1-7)	+19
2984	(1-8)	(1-8)	+39
3051	α	(1-6) + TA	+106
3129	β	(1-6) + LA	+184
3182	γ	(1-6) + 2TA	+237
3241	δ	(1-6) + TO	+296
3263	ϵ	(1-7) + TO	+318
3276	ζ	(1-6) + LO	+331
3293	η	(1-6) + 3TA	+348
3342	θ	(1-6) + TA + TO	+397
3474	ι	(1-6) + 2TA + TO	+529
3555	κ	(1-6) + 2TO	+610
3840	λ	(1-6) + 3TO	+895
Luminescence spectrum			
2927	(6-2)	(6-2)	−15[b]
2905	(6-3)	(6-3)	−37[b]
2891	(6-4)	(6-4)	−51[b]
2866		(6-5)	−76[b]
2836		TA + (6-1)	−106[b]
2800		TA + (6-2)	−142[b]
2635		TO + (6-1)	−307[b]
2620		TO + (6-2)	−322[b]
2590		LO + (6-1)	−352[b]
2563		LO + (6-2)	−379[b]

[a] Peak energies are those obtained at liquid-helium temperature for sample R139 (which had the lowest iron concentration and best resolved spectra of all the samples studied) and given in Tables II and IV of Slack, Ham, and Chrenko (Ref. 1) for the absorption spectrum and Table III of Slack and O'Meara (Ref. 2) for the luminescence. The values given in Table II of Ref. 1 have been reduced by 2 cm^{-1}, corresponding to the difference noted between the data for samples R114A and R139.

[b] Relative peak energies for all luminescence peaks have been shifted by 3 cm^{-1} on the assumption that luminescence peak (6-2) should coincide with absorption peak (2-6) and that the 3 cm^{-1} difference actually observed results from the different calibration of the two spectrometers used, as suggested in Ref. 2. Line (6-1) is not observed in luminescence because of reabsorption.

[c] These separations of levels 1–4 (Γ_1, Γ_4, Γ_3, and Γ_5 of ^5E, respectively) obtained from the near-infrared absorption agree well with the more accurate values obtained in Ref. 21 from far-infrared data: (1-2) = 15.0 cm^{-1}, (1-3) = 27.5 cm^{-1}, (1-4) = 45.0 cm^{-1}

pling with a totally symmetric Γ_1 (breathing) mode[47]], we conclude therefore that no prominent sideband corresponding to the emission of more than one phonon should appear in the absorption spectrum (contrast the SHC assignment given in Table III).

Second, the two prominent peaks labeled β and γ in the absorption spectrum in Fig. 5 are separated from (1-6) by frequencies which suggest from Table I that if they are one-phonon sidebands they might correspond to the emission of an LA phonon. Yet in this frequency interval in Fig. 6, 150–300 cm^{-1} from (1-6), there are no peaks at all in the luminescence. The absorption peaks β and γ thus cannot represent simple unshifted phonon sidebands of the (1-6) electronic transition since by our previous argument the appearance of such a sideband in the absorption would imply a similar sideband in the luminescence. Moreover, they cannot be simple zero-phonon lines since the Γ_5 level nearest to Γ_5 ($J' = 1$) expected from crystal-field theory (Fig. 1) should be $\sim 5|\lambda|$ higher, and this would be at least 350 cm^{-1}, even if covalency reduced $|\lambda|$ by as much as 30% from its free-ion value. To account for these absorption peaks we are therefore forced to appeal to some mechanism capable of causing a large relative shift in some of the absorption sidebands as compared with the corresponding sidebands in the luminescence. Since the only phonons affect-

ing the luminescence are evidently the TA, TO, and LO, we thus require a mechanism that can lead to the shifted absorption peaks via coupling with one or more of these modes. The Jahn-Teller coupling within the $^5T_2$ state is capable of causing such large relative shifts in the vibronic levels, as well as of shifting optical intensity to the one-phonon levels, as we have seen in Sec. IV, and we interpret the presence of these prominent shifted sidebands as evidence for the importance of such coupling. We will now explore this possibility in more detail.

Of course, we might account for differences in the sideband positions between the absorption and emission spectra by assuming that the relevant (local) vibrational modes have different frequencies corresponding to the different electronic charge distributions in the ^5E and $^5T_2$ states. The fact that the luminescence sidebands correspond well with the phonon frequencies of the ZnS lattice in Table I indicates that such local-mode frequency shifts are not important in the ^5E states, and we may therefore suppose that they should be of no greater importance in the $^5T_2$ state. Moreover, if such frequency shifts come about from a second-order correction to the energy as a result of the electron-phonon interaction (5) coupling a given electronic level to distant levels[48] (a process emphasized recently by Pearson[49] and called by him the "second-order Jahn-Teller effect"), the corresponding change in the force constant $\mu\omega^2$ in Eq. (6) is proportional to the ratio of an electron-phonon interlevel coupling energy, related to the coupling coefficient $V_\rho(i)$ in analogy to E_{JT} in Eq. (10), to the electronic energy-level separation. For this frequency shift to be large, this interlevel coupling energy would have to be comparable to the level separation. This, of course, is a possibility, but if this electron-phonon *inter*level coupling were so strong, it would seem likely that the Jahn-Teller energy for *intra*level coupling might be equally large. Since for Fe^{2+} in ZnS the Jahn-Teller energy in $^5T_2$ is at most several hundred cm^{-1} (and considerably less in ^5E), while level separations are very much larger, we will assume that such frequency shifts from coupling to other electronic states are unimportant in this case.

In accounting for the appearance of one Γ_5 vibronic level about 200 cm^{-1} above the Γ_5 ($J'=1$) ground state of $^5T_2$ (we recall that electric-dipole transitions from the Γ_1 level of ^5E are allowed only to Γ_5 levels), we have seen in Fig. 2 that we obtain such a shifted level from Jahn-Teller coupling with a Γ_3 mode of frequency $\hbar\omega_E^B \sim 300$ cm^{-1} if we have $E_{JT}^B \sim 130$ cm^{-1}. This level arises from the Γ_5 ($J'=1$) electronic state with the excitation of one vibrational quantum, and it is then depressed in energy by the Jahn-Teller coupling. A similarly depressed one-phonon Γ_5 level would be obtained if the Jahn-Teller coupling were with a Γ_5 mode of frequency ~ 300 cm^{-1}. However, in order to get two such levels to account for *both* absorption peaks β and γ, it may not suffice simply to assume Jahn-Teller coupling to two independent modes with frequency near 300 cm^{-1} since interaction between the two resulting one-phonon Γ_5 levels may lead only one of these to be strongly depressed. (This is clear if two modes having the same frequency are both Γ_3 or both Γ_5 since we can then form linear combinations such that the Jahn-Teller coupling is with one mode only. Nevertheless, we have seen in Fig. 4 that we can get two Γ_5 levels depressed into the region 150–250 cm^{-1} above Γ_5 ($J'=1$) if we assume simultaneous coupling to a second mode having a frequency ~ 100 cm^{-1}. We see therefore that we can account qualitatively for the appearance of the two shifted absorption peaks β and γ, on the basis of simultaneous Jahn-Teller coupling to two groups of phonons having frequencies agreeing with the TA and TO + LO groups appearing in the luminescence. [To obtain Γ_5 levels 184 and 237 cm^{-1} (Table III) above Γ_5 ($J'=1$) on the basis of the assumptions of Fig. 4, it would appear we would need $E_{JT}^A \sim 200$ cm^{-1}, $E_{JT}^B \sim 100$ cm^{-1}, and in addition a value for $|\lambda|$ slightly reduced by covalency from its free-ion value in order to bring the Γ_5: (Γ_4, $J'=2$) + A level a bit lower.]

If there is Jahn-Teller coupling with a mode of frequency ~ 100 cm^{-1}, we are led on the basis of Figs. 3 and 4 [or Eqs. (A9) and (A10)] to expect one or more Γ_5 levels to be depressed to within an energy interval from the Γ_5 ($J'=1$) ground state which could be quite small. These levels in appropriate circumstances may simulate the vibrational levels of a simple harmonic oscillator of very low frequency. However, as discussed in Sec. IV and seen also in Table II, these excited levels are coupled only very weakly with the Γ_5 ($J'=1$) zero-phonon state, so that transitions to these levels do not borrow much optical intensity unless the levels are very close to Γ_5 ($J'=1$). There may be evidence of such levels in the very weak absorption lines (1-7) and (1-8) (Fig. 5 and Table III), which, as noted by SHC, seem to be part of the Fe^{2+} spectrum since they are present in all the samples studied and have also been seen by other workers.[50] Clearer evidence of such levels is however found in the absorption spectrum of Fe^{2+} in CdTe (see Figs. 6 and 7 of Ref. 1), for which lines (1-7) and (1-8) were found to have intensity of the same size as that of (1-6). Since CdTe has substantially lower frequencies[51] for the TA branch of the phonon spectrum than does ZnS, it would not be surprising that the Jahn-Teller coupling leads to a more nearly equal distribution of the optical intensity among the low-energy vibronic states in this case than is found in ZnS.

If we attribute the absorption peaks β and γ to

Jahn-Teller coupling to the TA and TO + LO groups of phonons, how may we account for the remaining weaker peaks labeled α, δ, ϵ, ζ, and η in Fig. 5, which are separated from line (1-6) by intervals (Table III) which agree fairly well with various phonon energies of ZnS listed in Table I? Some of these peaks δ, ϵ, ζ, and η may, of course, result from weaker Jahn-Teller coupling with other TO or LO modes (for example, the Γ_5 modes, if the dominant Jahn-Teller coupling is with Γ_3 modes), or from transitions to higher levels of the vibronic sequence that contains β and γ. Another possibility is that some of these sidebands arise from differences in the coupling of the ^5E and $^5T_2$ states to totally symmetric vibrations.[52,53] Such breathing modes, having Γ_1 symmetry, represent independent linear combinations of, say, the LO(X) phonons, different from the Γ_3 and Γ_5 modes that participate in the Jahn-Teller coupling. They therefore can contribute separate sidebands, which should be displaced from the zero-phonon lines by exactly the mode frequency, since a totally symmetric distortion displaces all the states of $^5T_2$ (or ^5E) by the same amount and thus causes no relative shift of any of the $^5T_2$ vibronic levels. We expect, of course, that there should be some such coupling with the Γ_1 modes[54] (thus reflecting the difference in the equilibrium position for this mode of distortion between the ^5E and $^5T_2$ states) because we expect that the cubic-field splitting $\Delta = 10|Dq|$ depends on crystal volume. We find from Table I that whereas TA(X) and TA(L) do not give rise to a Γ_1 mode, we do have such a mode from the region of the maximum in the TA branch near K. Since phonons over a broad region near K probably contribute more or less equivalently, this mechanism would seem a plausible one to account for the peak α in Fig. 5. Similarly, the TO branch also contributes a Γ_1 mode from the region near K, and this region should correspond roughly to the strong peak in the phonon density of states expected (Sec. III) from this branch. Such a Γ_1 mode might therefore account for the peak δ, which at 296 cm^{-1} falls in this range. Finally, we have Γ_1 modes from LO(X) and LO(L), so that Γ_1 modes from the LO branch may account for one or more of the weaker peaks ϵ, ζ, and η.

Alternatively, we may obtain one-phonon sidebands of the $[\Gamma_1\,{}^5E \rightarrow \Gamma_5(J'=1)^5T_2]$ transition by borrowing optical intensity in the usual way[52,53,55-57] from allowed electronic transitions of much higher energy, through the electron-phonon interaction. Such phonon-assisted transitions come about via a second-order process involving the interaction of the electrons with the light, on one hand, and the terms in Eq. (5) that couple ^5E and $^5T_2$ to these distant electronic states, on the other. Such sidebands of the $[\Gamma_1\,{}^5E \rightarrow \Gamma_5(J'=1)^5T_2]$ transition may, in principle, be allowed for any phonon of symmetry Γ_1, Γ_3, Γ_4, and Γ_5, so that unshifted one-phonon sidebands that borrow intensity in this way are possible for many additional phonons that do not participate in the Jahn-Teller coupling. We might expect to find sidebands having this origin in our spectra, since all optical transitions within the $3d^6$ configuration of the Fe^{2+} would otherwise be (electric-dipole) forbidden if the Fe^{2+} were in a site having inversion symmetry, and it is this mechanism which is the usual one[55-57] that makes such transitions allowed via the vibrational coupling.

Of the phonons at symmetry points listed in Table I, all of those contributing a mode of symmetry Γ_3 or Γ_5 may, in principle, participate in the Jahn-Teller coupling within $^5T_2$. It is tempting to speculate, however, that the Jahn-Teller coupling occurs mainly with the Γ_3 modes. The TA(L) mode at 70 cm^{-1} [as well as the TA(K) modes at 90 and 125 cm^{-1}] then provides a low-frequency mode suitable for the interpretation we have proposed, while the LO and TO branches would provide a Γ_3 mode near 300 cm^{-1} [for example, LO(X), TO(L), or either branch near K]. Coupling with the TA(L) mode would moreover account for the weak luminescence line labeled (6-5) by Slack and O'Meara[2] in Table III [the (6-5) transition should not be allowed as a zero-phonon line]. Weak Jahn-Teller coupling with the Γ_5 modes would then be consistent with the absence of any evident coupling with the LA(X) or LA(L) phonons. As noted in Sec. III, however, LA(X) involves motion only on the Zn sites, and as we expect the Jahn-Teller coupling for an Fe^{2+} ion on a Zn site to be strongest with those modes having an even component of displacement on the nearest-neighbor S sites, this explanation alone probably suffices to account for weak coupling with LA(X). Finally, we know from studies[58] of Cr^{2+} in ZnS, ZnSe, ZnTe, and other II-VI compounds that the predominant Jahn-Teller coupling in the $^5T_2$ ground state is with a Γ_3 mode and that this coupling is strong enough to lead to a static Jahn-Teller distortion. The similarity of the corresponding electronic states of Cr^{2+} and Fe^{2+} in terms of the complementary relationship between holes and electrons in the $3d$ shell (Fe^{2+} has six electrons, Cr^{2+} six holes) leads us to expect that the Jahn-Teller coupling of these ions in similar environments should not be wholly dissimilar. Therefore, we should expect that the Γ_3 coupling in the $^5T_2$ state of the Fe^{2+} should predominate, even though it is evidently not so strong for Fe^{2+} as for Cr^{2+}.

One quantitative check on our interpretation is provided by the value 535 cm^{-1} which SHC[1] obtained for what they interpreted as the apparent Jahn-Teller energy in the $^5T_2$ state. This was given by the difference between the energy of the (1-6) transition and the average electronic energy of the $^5T_2$

states in the equilibrium lattice configuration appropriate to ^5E, relative to the Γ_1 level of ^5E, as given by the moment ratio (M_1/M_0) of the optical absorption spectrum as defined by SHC. In the strong-coupling model of SHC, this difference is the sum of the true Jahn-Teller energy and the amount by which the $^5T_2$ states in equilibrium are lowered relative to the ^5E equilibrium energy by the difference in the coupling of these states to totally symmetric vibrational modes. Since this moment ratio is independent of the Jahn-Teller coupling[1,4] (so long as we can neglect such coupling within ^5E), it provides an equally valid reference energy for our revised interpretation.[59] In our present weak-coupling model, however, starting from the static crystal-field model, we see that the lowest $^5T_2$ level Γ_5 $(J'=1)$ lies below the average energy of the $^5T_2$ states by the spin-orbit energy difference $\sim 3|\lambda|$. This level is then lowered further by the Jahn-Teller coupling and by the coupling to the totally symmetric modes. Using the model of the Appendix with Jahn-Teller coupling to two Γ_3 modes of frequency (A) 100 and (B) 300 cm^{-1}, we have $\Delta E_{JT} = 0.200\, E_{JT}^A + 0.415\, E_{JT}^B$ (weak-coupling approximation) for this Jahn-Teller shift from Eq. (A3a). Thus for $E_{JT}^A \sim 200$ cm^{-1}, $E_{JT}^B \sim 100$ cm^{-1} we should have $\Delta E_{JT} \sim 80$ cm^{-1}, so that using $3|\lambda| \sim 300$ cm^{-1} we would leave a shift $\Delta E_A \sim 155$ cm^{-1} to be supplied by the Γ_1 coupling in order to make up the full difference of 535 cm^{-1}. This value for ΔE_A may be compared with the value inferred from the intensity of the sidebands in the absorption spectrum which we attribute to coupling to Γ_1 modes. Since Eq. (9) gives the intensity distribution[47] for coupling to a Γ_1 mode if we replace S_E by $S_A^i = \Delta E_A^i/\hbar\omega_A^i$, where ΔE_A^i is that part of ΔE_A attributed to the ith Γ_1 mode, we find that the ratio of the integrated intensity of the one-phonon sideband to that of the zero-phonon line from which it is derived is given by

$$p_1^i/p_0 = S_A^i \,. \tag{14}$$

We can therefore use this formula for those sidebands of the (1-6) line in the absorption spectrum of Fig. 5 which we have suggested may be due to coupling to the Γ_1 modes. Since the peak α, which corresponds to $\hbar\omega = 106$ cm^{-1}, has roughly one-quarter the integrated intensity of the (1-6) line, we obtain ~ 25 cm^{-1} as the contribution to ΔE_A from the coupling to this mode. The peaks δ, ϵ, ζ, and η corresponding to $\hbar\omega \sim 300$ cm^{-1} together have roughly the same intensity as (1-6); ascribing half of this to Γ_1 coupling, we obtain ~ 150 cm^{-1} for their contribution to ΔE_A. The sum of these contributions then would compare reasonably well with the value 155 cm^{-1} obtained previously.

A further check on our interpretation is provided by the second moment $\langle E^2\rangle = (M_2 - M_1^2)M_0^{-1}$ of the full $^5E \rightarrow {}^5T_2$ absorption spectrum of Fig. 5. Using the methods of Henry, Schnatterly, and Slichter,[4] and assuming negligible Jahn-Teller coupling within the ^5E states, we may show that when the initial state is the Γ_1 level of ^5E (0 °K spectrum) we have

$$\langle E^2\rangle = 6\lambda^2 + \textstyle\sum_i S_E^i(\hbar\omega_E^i)^2 + \frac{3}{2}\sum_i S_T^i(\hbar\omega_T^i)^2 + \sum_i S_A^i(\hbar\omega_A^i)^2 \,. \tag{15}$$

Here S_A^i, S_E^i, and S_T^i are the Huang-Rhys parameters, which describe the coupling of the $^5T_2$ states to the ith Γ_1, Γ_3, and Γ_5 modes, respectively, and are defined as in Eq. (11).[60] The excess of the second moment over the expected spin-orbit contribution thus provides a measure of the total strength of the coupling of the $^5T_2$ states to the phonons, and this is independent of the details of the structure of the spectrum. We find for the experimental spectrum of Fig. 5 the value $\langle E^2\rangle = 12\times10^4$ cm^{-2}. The model in the Appendix with the two modes A and B, for $E_{JT}^A \sim 200$ cm^{-1}, $E_{JT}^B \sim 100$ cm^{-1}, would yield from Eq. (15) a value $\sim 5\times10^4$ cm^{-2} for the combined contribution to $\langle E^2\rangle$ of the Jahn-Teller coupling to the Γ_3 modes, while the preceding estimate of the coupling to the totally symmetric modes yields $\sim 5\times10^4$ cm^{-2} for the contribution from the Γ_1 coupling. Since we have the free-ion value $6\lambda^2 = 6\times10^4$ cm^{-2}, this model thus yields an estimate $\langle E^2\rangle \sim 16\times10^4$ cm^{-2}. This is somewhat larger than the experimental value, the discrepancy suggesting that the model either overestimates the coupling to some of the modes or that a smaller value of λ may be more appropriate as the result of covalency. The experimental value of $\langle E^2\rangle$ is in any case not consistent with a model in which a Jahn-Teller coupling much stronger than the spin-orbit interaction is postulated. We note that Eq. (15) does not provide a means of distinguishing between coupling to Γ_3 and Γ_5 modes, so that we still have no basis for ruling out the possibility that part of the Jahn-Teller coupling may be with one or more Γ_5 modes.

The second moment of the luminescence spectrum in Fig. 6 is very much smaller than that of the absorption [and is harder to determine because of reabsorption in the vicinity of the (1-6) line], and this difference is again consistent with our interpretation. Since the initial state for the luminescence is the Γ_5 $(J'=1)$ ground state of $^5T_2$, and since for weak Jahn-Teller coupling this state gives rise only to very weak sideband intensities for Γ_3 and Γ_5 modes in the luminescence, as seen in Table II, the contribution of the Jahn-Teller coupling to $\langle E^2\rangle$ should be very much reduced in luminescence as compared to absorption (assuming still that Jahn-Teller coupling within ^5E is negligible). The contribution of Γ_1 coupling to $\langle E^2\rangle$, on the other hand, should be the same in luminescence as

in absorption, since it is the difference between the ^5E and $^5T_2$ states in the linear coupling to such modes that leads to the sideband intensity, and since this coupling is the same for all the spin-orbit levels of $^5T_2$. The second moment of the luminescence therefore provides an upper bound for the contribution of Γ_1 coupling to $\langle E^2 \rangle$ in absorption, thus confirming our interpretation that the Jahn-Teller coupling causes a large part of the broadening of the absorption spectrum.

An upper bound to the fraction of the total optical intensity of the $^5E \rightarrow {}^5T_2$ band at 0 °K which is borrowed through the electron-phonon interaction from other allowed electronic transitions is provided by the temperature variation of the total intensity. In the absence of such borrowing, the zeroth moment M_0 of the spectrum is independent of temperature,[4] but if such a contribution is present as a result of coupling with a mode of frequency ω it may be shown[9] that this part of M_0 varies as

$$\Delta M_0(T) = \Delta M_0(0) \coth(\hbar\omega/2kT) . \qquad (16)$$

Since the total intensity of the $^5E \rightarrow {}^5T_2$ band was found[61] to increase by only ~ 5% from 0 to 300 °K, we find from Eq. (16) that $\Delta M_0(0)$ could account for ~ 9% of M_0 at 0 °K if the coupling involved a mode of frequency ~ 300 cm^{-1}, or only ~ 2% for a mode ~ 100 cm^{-1}. Such borrowed contributions to the intensity do not therefore appear to play a major role in the spectra of Figs. 5 and 6, although they might still be responsible for some of the smaller features observed in the sideband structure.

Other checks on the interpretation can, in principle, be obtained from the intensities of the sideband peaks attributed to the Jahn-Teller modes, using the theoretical predictions such as those of Table II. However, the inaccuracy of our perturbation treatment is too great, for the vibronic levels with one or more phonons excited, to make such a comparison meaningful in the absence of more elaborate calculations of the vibronic states. The observed peak intensities in Fig. 5, however, do not appear to be inconsistent with those expected on the basis of Table II. Similar comparisons of the sideband intensities in the luminescence with the theory (Table II) are possible but are not particularly enlightening because of the difficulty in sorting out the several overlapping contributions to these peaks.

Finally, we should note that in our revised interpretation, we attribute the peaks θ, ι, κ, and λ in the absorption spectrum lying higher than ~ 3300 cm^{-1} to transitions to the levels derived from the zero-phonon Γ_5 ($J' = 3$) state and the excited phonon states associated with $J' = 2$ and 3. We do not attempt a detailed interpretation of these peaks, apart from noting that their strength of course reflects the strength of the second zero-phonon transition [$\Gamma_1 {}^5E \rightarrow \Gamma_5 (J' = 3) {}^5T_2$] expected from Fig. 1 on the basis of crystal-field theory.

VI. Fe^{2+} IN OTHER CRYSTALS

The $^5E \rightarrow {}^5T_2$ absorption spectrum of tetrahedrally coordinated Fe^{2+} in a number of other crystals is quite similar to that of Fe^{2+} in ZnS. Luminescence spectra are not available for most of these crystals, and we will not attempt a detailed interpretation for any of them. Nevertheless, it appears likely from the available evidence that dynamic Jahn-Teller effects like those we have described for the ZnS are important also in these other cases.

We have already mentioned that the appearance (see Figs. 6 and 7 of SHC) of two additional strong absorption peaks in CdTe within 30 cm^{-1} of the (1-6) zero-phonon line, a result that could not be accounted for either by crystal-field theory or by the phenomenological model for a strongly coupled Jahn-Teller system advanced by SHC, finds a ready explanation in the dynamic Jahn-Teller effect if coupling is with a mode of low frequency. Since the TA branch of CdTe has a lower frequency than the corresponding phonons of any other II-VI or III-V compound for which the phonon spectrum is known,[51] we might expect the effect of coupling to this mode to be more pronounced for CdTe than for the other crystals, as is evidently the case.[16] Also, the small value of 255 cm^{-1} found by SHC[1] for the apparent Jahn-Teller energy in CdTe is consistent with a weak dynamic coupling but too small to be compatible with a strongly coupled model. Consistent with this interpretation, the second moment of the absorption spectrum is very much smaller than in ZnS.

In spinel, $MgAl_2O_4$, there are probably no critical points in the phonon spectrum with energy smaller than ~ 200 cm^{-1},[1] so that there is in this case no low-frequency mode to which coupling might occur. The nearest peak in the absorption spectrum to the (1-6) zero-phonon line is the line (1-7) lying 65 cm^{-1} above (1-6). While this separation is much too small to be accounted for by crystal-field theory, this peak could well be the result of a transition to a Γ_5 level which is derived from the Γ_5 ($J' = 1$) electronic state via the excitation of one phonon of 200–300 cm^{-1} and which is then depressed in energy by the Jahn-Teller coupling, like the one-phonon Γ_5 level of Fig. 2. We can estimate from Fig. 2 that for this level to be brought to 65 cm^{-1} from the Γ_5 ($J' = 1$) level we must have a value for E_{JT} in the range 300–400 cm^{-1} for the coupling to this mode. This is somewhat larger than the values we estimated for ZnS; however, SHC did obtain a value of 945 cm^{-1} for the apparent Jahn-Teller energy in $MgAl_2O_4$ which would be consistent with this larger estimate, and the second moment of the absorption

is significantly larger than for ZnS, indicating from Eq. (15) a stronger phonon coupling in spinel.

The absorption spectra of Fe^{2+} in ZnSe, ZnTe, CdS, GaP, and GaAs at liquid-helium temperature measured by Baranowski, Allen, and Pearson[16] all show the sharp zero-phonon lines resulting from the (1-6), (2-6), etc., transitions at the low-energy edge of the spectrum. At higher energy there are additional peaks which in several cases (e.g., ZnSe, CdS, and ZnTe) resemble those in ZnS or CdTe quite closely, and the over-all widths of the absorption band are similar. One infers that the coupling to the phonons in all these cases may be similar to that in ZnS. Unfortunately, however, we do not have for these crystals the corresponding information from the luminescence spectra that we had for ZnS to enable us to tell to which phonon the Fe^{2+} is coupled and thus to identify those peaks which are shifted by the Jahn-Teller coupling. Only for ZnSe is the Fe^{2+} luminescence spectrum available, from the work of Haanstra,[17] and in this case the phonon peaks in the luminescence do not separate into clearly distinguishable groups as they did in ZnS, possibly because a stronger coupling to a TA mode in ZnSe produces sidebands corresponding to the excitation of more than one TA phonon.

VII. DISCUSSION

In the present work, we have seen an example of the way in which dynamic Jahn-Teller effects may modify the optical absorption and luminescence spectra of an ion or complex in a crystal by not only partially quenching the crystal-field and spin-orbit splittings of zero-phonon levels but also splitting, shifting, and mixing the associated vibrational levels. For the case of Fe^{2+} in ZnS, we have considered in some detail how the Jahn-Teller coupling may transfer optical intensity to the vibronic sidebands and shift these relative to the zero-phonon lines in the manner required to account for the observed spectra. We have shown that, whereas the Jahn-Teller coupling cannot be as strong for this ion as originally supposed by SHC,[1] the large shifts of some of the sideband peaks in absorption provide persuasive evidence of the important role played by dynamic Jahn-Teller effects in these spectra. This interpretation is confirmed by a comparison of the second moments of the absorption and luminescence spectra. We have proposed a model which accounts qualitatively for the principal features of the observed spectra by postulating Jahn-Teller coupling with two groups of phonons, one with frequency ~100 cm^{-1} from the TA branch of the ZnS lattice spectrum, and the other from the TO and LO branches ~300 cm^{-1}. While we have speculated that this coupling may be predominantly with modes having Γ_3 symmetry, we have not been able to distinguish with any certainty between the various possible phonons which may be involved, and we cannot rule out the possibility that this coupling may be partly or even predominantly with Γ_5 modes. In addition, there is evidence of significant but rather weak coupling with totally symmetric Γ_1 modes, which contribute additional structure to the spectrum.

The role of a dynamic Jahn-Teller effect in splitting and shifting vibronic levels with one or more vibrational quanta excited has been recognized since the pioneer work in this field by Moffitt and Liehr[10] and Longuet-Higgins *et al.*,[12] but there has been more attention paid to this in the study of molecules than in work on the spectra of defect centers in solids. In particular, Weinstock and Goodman[13] have given a detailed interpretation of unusual infrared and Raman spectra of the hexafluoride molecules on this basis, while Herzberg has included a good discussion of Jahn-Teller effects in the vibrational structure of electronic transitions in molecules in his book.[9] In solids, on the other hand, vibrational spectra are more complex than in molecules, and our knowledge of vibrational modes associated with defect centers is rather limited; therefore, it is usually difficult to identify the detailed structure of the sidebands in optical spectra of defects with the effects of Jahn-Teller coupling on individual vibronic levels. The recent blossoming of interest in dynamic Jahn-Teller effects in optical spectra of impurity ions in solids[5] has therefore focused, on one hand, on the zero-phonon lines and the partial Jahn-Teller quenching of the splitting of these lines due to crystal-field and spin-orbit interactions, magnetic fields, applied stress, etc.[3,8] On the other hand, attention has been directed to the broad optical absorption bands of strongly coupled Jahn-Teller systems, in which certain features in the shape of the bands (e.g., broad double or triple peaks) have been shown by O'Brien, Moran, Toyozawa, Cho, Englman, and others[6,62-65] to be the result of the Jahn-Teller coupling. Nevertheless, as the present work shows and as is also seen in some other studies, for example, that of Fetterman and Fitchen[66] of the R' center in LiF, it is *sometimes* possible to identify the effects of Jahn-Teller coupling on the detailed fine structure of the vibrational sidebands of the optical spectra of defect centers in crystals. For this identification to be possible, this vibrational fine structure must, of course, be resolved, together with the zero-phonon lines, and the Jahn-Teller effects (e.g., the relative shifts of the vibronic levels) must be sufficiently large. Such effects appear always to be characterized by major departures from "mirror" symmetry in the vibrational structure of corresponding low-temperature absorption and emission spectra relative to the zero-phonon lines.

One particularly interesting aspect of the present work from the viewpoint of the general theory of the Jahn-Teller effect is the insight it provides into the relationship between the phonons of the host crystal and the localized modes that are primarily responsible for the Jahn-Teller effects in strongly coupled systems. For weak coupling, it is clear from our present work and on general principles that many different lattice modes that have the correct symmetry may participate in the Jahn-Teller coupling. Yet it has by now been quite well documented[5,46] that strongly coupled systems behave as though the Jahn-Teller coupling were predominantly with a single mode, which is often represented as being a mode of vibration of the cluster of ions consisting of the Jahn-Teller ion and its nearest neighbors, embedded in the elastic medium of the host crystal. Though this cluster continues to be dynamically coupled to the rest of the lattice, this coupling is often relatively weak and can be viewed as a perturbation on the cluster, serving primarily to induce transitions, via the absorption or emission of a lattice phonon, between the vibronic levels of the much more strongly coupled cluster. We can now begin to see in outline how this latter situation develops as the strength of the Jahn-Teller coupling increases, as follows. We have seen in Sec. IV that in weak coupling, for which our perturbation treatment is appropriate, there is a second-order coupling between vibronic states of the same overall symmetry which however represent the excitation of different phonons. As a result of this coupling, the actual vibronic eigenstates of the system are admixtures of these states. In the case in which we have Jahn-Teller coupling with several phonons of similar frequency, or with a band of phonons, this second-order coupling serves thus to select a linear combination of these modes that maximizes the Jahn-Teller coupling, and it is the vibronic states associated with this combination mode that are displaced in energy (as in Fig. 2) by the Jahn-Teller coupling. Alternatively, if the Jahn-Teller coupling is with a number of modes of rather different frequencies, this second-order coupling (or higher-order coupling as the coupling strength increases) again mixes the vibronic states, and when the Jahn-Teller energy is larger than the difference in $\hbar\omega$ the low-energy vibronic eigenstates of the system are again those mixed states which maximize the Jahn-Teller coupling. We see therefore that there is no necessary relationship between the apparent frequency of the effective mode which dominates the Jahn-Teller coupling in the strongly coupled case, on one hand, and the frequencies of individual phonons of the unperturbed lattice, on the other, unless the phonons that couple strongly lie in a well-defined band. We see, moreover, why the cluster model often works: Since the Jahn-Teller coupling with lattice distortions should ordinarily be strongest with displacements of the nearest neighbor ions, it is precisely a mode of this cluster that maximizes the Jahn-Teller coupling and thus is selected in the strong-coupling limit even though this mode is not a normal mode of vibration of the unperturbed lattice.

Further experimental tests of our interpretation of the optical spectrum of Fe^{2+} in ZnS are clearly desirable. One such test, which could check the identification of the various sideband peaks in the 0 °K spectrum and distinguish whether the Jahn-Teller coupling is predominantly with Γ_3 or Γ_5 modes, would be a study of the magnetic circular dichroism of these peaks and of their linear dichroism under applied stress. As Henry, Schnatterly, and Slichter have shown,[4] it is possible to obtain from the change in the first moment of the dichroism of the full absorption band the unquenched coupling coefficients that describe the splitting of the electronic levels in the crystal field of the rigid lattice in a magnetic field or under stress. The splitting of the zero-phonon lines, on the other hand, or the dichroism in these peaks if a splitting is not resolved,[67] determines these coupling coefficients for the vibronic levels, reduced by the appropriate Jahn-Teller reduction factors. Merle d'Aubigné and Roussel[68] have indeed very recently used a comparison of the results of these two types of measurements of circular dichroism to determine directly the reduction factor for the spin-orbit interaction in the $^2T_{1u}$ excited state of the F^+ center in CaO. In the present case for Fe^{2+} in ZnS, since the initial state for the 0 °K absorption spectrum is the Γ_1 singlet level of ^5E, the dichroism in the (1-6) line would measure directly the Zeeman or stress splitting of the Γ_5 ($J'=1$) level of $^5T_2$ as modified by the appropriate reduction factors. The comparison of the results of such measurements with the theory of these reduction factors, which depend on the strength and type of Jahn-Teller coupling, would, of course, then provide one test of our interpretation just as in the corresponding treatment of Fe^{2+} in MgO by Ham, Schwarz, and O'Brien.[7] In the sideband structure, a peak derived from the zero-phonon line by the excitation of one totally symmetric Γ_1 mode should have exactly the same dichroism as the (1-6) line. Peaks associated with the higher vibronic levels of the Jahn-Teller active modes will, however, in most cases have a different dichroism, since such levels mix the electronic states with $J'=1$, 2, 3 in different ways. Such studies of the dichroism thus would offer a direct means of identifying the type of mode involved in a sideband peak and would enable one to develop a more detailed model of the Jahn-Teller coupling with the various Γ_3 and Γ_5 modes than is possible on the basis of the simple absorption and

luminescence data alone.

APPENDIX: JAHN-TELLER SHIFTS OF VIBRONIC ENERGY LEVELS: PERTURBATION TREATMENT OF $^5T_2$ STATE OF Fe^{2+} COUPLED TO TWO Γ_3 MODES

As in the work of Ham, Schwarz, and O'Brien,[69] we treat the Jahn-Teller coupling as a perturbation on the vibronic eigenstates of

$$\mathcal{H}_0 = \mathcal{H}_{so} + \mathcal{H}_{lat} \ . \tag{A1}$$

In the spin-orbit interaction $\mathcal{H}_{so}$ for the $^5T_2$ state [Eq. (2)] we drop for simplicity the small terms in μ and η, so that we ignore the splitting within the $J' = 2$ and 3 levels of Fig. 1. $\mathcal{H}_{lat}$ is given by Eq. (6). The Jahn-Teller interaction with two Γ_3 modes, having frequencies ω_E^A and ω_E^B and coupling coefficients V_E^A and V_E^B, respectively, is described [Eq. (7)] by

$$\mathcal{H}_{JT} = V_E^A(Q_\theta^A \mathcal{S}_\theta + Q_\epsilon^A \mathcal{S}_\epsilon) + V_E^B(Q_\theta^B \mathcal{S}_\theta + Q_\epsilon^B \mathcal{S}_\epsilon) \ . \tag{A2}$$

This coupling displaces the eigenstates of $\mathcal{H}_0$, and in second-order perturbation theory we obtain for the energy shifts of the zero-phonon ground state Γ_5 $(J' = 1)$ and lowest excited spin-orbit states Γ_3, Γ_4 $(J' = 2)$ the results[69,70]

$$\Delta E(\Gamma_5;\ \Gamma_5,\ J' = 1;\ 0_A, 0_B) = -\sum_{j=A,B} E_{JT}^j F_1(\zeta, \omega_E^j) \ , \tag{A3a}$$

$$\Delta E(\Gamma_3;\ \Gamma_3,\ J' = 2;\ \ 0_A, 0_B) = -\sum_{j=A,B} E_{JT}^j F_2(\zeta, \omega_E^j) \ , \tag{A3b}$$

$$\Delta E(\Gamma_4;\ \Gamma_4,\ J' = 2;\ 0_A, 0_B) = -\sum_{j=A,B} E_{JT}^j F_3(\zeta, \omega_E^j) \ . \tag{A3c}$$

Here E_{JT}^A and E_{JT}^B are given in terms of V_E^A, V_E^B, ω_E^A, and ω_E^B by Eq. (10), and the $F_n(\zeta, \omega)$ are functions which have been defined previously [Ref. 7, Eq. (2.15)].

The second-order displacements of the Γ_4 and Γ_5 levels derived from the lowest electronic level Γ_5 $(J' = 1)$ but with one A quantum excited may be expressed in terms of the shift (A3a) of the ground state as

$$\Delta E(\Gamma_5;\ \Gamma_5,\ J' = 1;\ 1_A, 0_B)$$

$$= \Delta E(\Gamma_5;\ \Gamma_5,\ J' = 1;\ 0_A, 0_B) - E_{JT}^A I_1(\zeta, \omega_E^A) \ , \tag{A4a}$$

$$\Delta E(\Gamma_4;\ \Gamma_5,\ J' = 1;\ 1_A, 0_B)$$

$$= \Delta E(\Gamma_5;\ \Gamma_5,\ J' = 1;\ 0_A, 0_B) - E_{JT}^A I_2(\zeta, \omega_E^A) \ , \tag{A4b}$$

where

$$I_1(\zeta, \omega) = \tfrac{27}{5}\, \zeta\hbar\omega/[(5\zeta)^2 - (\hbar\omega)^2] \ , \tag{A5a}$$

$$I_2(\zeta, \omega) = \tfrac{3}{5}\, \zeta\hbar\omega/[(2\zeta)^2 - (\hbar\omega)^2] + 3\zeta\hbar\omega/[(5\zeta)^2 - (\hbar\omega)^2] \ . \tag{A5b}$$

The shifts of the corresponding levels having one B quantum excited may be obtained from Eq. (A4) by interchanging A and B.

We will also be interested in the Γ_4 and Γ_5 levels derived from the Γ_4 $(J' = 2)$ electronic level by the excitation of one A quantum. We have for the shifts of these levels

$$\Delta E(\Gamma_5;\ \Gamma_4,\ J' = 2;\ 1_A, 0_B)$$

$$= \Delta E(\Gamma_4;\ \Gamma_4,\ J' = 2;\ 0_A, 0_B) - E_{JT}^A I_3(\zeta, \omega_E^A) \ , \tag{A6a}$$

$$\Delta E(\Gamma_4;\ \Gamma_4,\ J' = 2;\ 1_A, 0_B)$$

$$= \Delta E(\Gamma_4;\ \Gamma_4,\ J' = 2;\ 0_A, 0_B) - E_{JT}^A I_4(\zeta, \omega_E^A) \ , \tag{A6b}$$

where

$$I_3(\zeta, \omega) = -\tfrac{3}{5}\, \zeta\hbar\omega/[(2\zeta)^2 - (\hbar\omega)^2] + \tfrac{3}{5}\zeta\hbar\omega/[(3\zeta)^2 - (\hbar\omega)^2] \ , \tag{A7a}$$

$$I_4(\zeta, \omega) = 3\, \zeta\hbar\omega/[(3\zeta)^2 - (\hbar\omega)^2] \ . \tag{A7b}$$

If $\hbar\omega_E^A$ is small compared with the spin-orbit splitting 2ζ between the lowest electronic levels, we may show that the relative energies of *all* the vibronic states of the A mode derived from the Γ_5 $(J' = 1)$ electronic ground state, for any number of excited quanta, are the same as those of the effective Hamiltonian

$$\mathcal{H}_{eff} = (2\mu)^{-1}[P_\theta^2 + P_\epsilon^2 + (\mu\omega_E^A)^2 (Q_\theta^2 + Q_\epsilon^2)]$$

$$+ \tfrac{1}{10}\, V_E^A(Q_\theta \mathcal{S}'_\theta + Q_\epsilon \mathcal{S}'_\epsilon) - \tfrac{243}{2000}\, [(V_E^A)^2/\zeta]\, (Q_\theta^2 + Q_\epsilon^2)$$

$$+ \tfrac{27}{2000}\, [(V_E^A)^2/\zeta][\mathcal{S}'_\theta(Q_\epsilon^2 - Q_\theta^2) + \mathcal{S}'_\epsilon(2Q_\theta Q_\epsilon)] \ , \tag{A8}$$

again to the accuracy of treating the Jahn-Teller coupling to the higher spin-orbit states by second-order perturbation theory. In Eq. (A8), $\mathcal{S}'_\theta$ and $\mathcal{S}'_\epsilon$ are the same electronic operators as $\mathcal{S}_\theta$ and $\mathcal{S}_\epsilon$ in Eq. (8), except that $\mathcal{S}'_\theta$ and $\mathcal{S}'_\epsilon$ are defined with respect to the Γ_5 $(J' = 1)$ spin-orbit triplet instead of the orbital Γ_5 triplet. Since $\mathcal{S}'_\theta$ and $\mathcal{S}'_\epsilon$ are diagonal with respect to the states $\Gamma_5\xi$, $\Gamma_5\eta$, and $\Gamma_5\zeta$ (and we have $\langle \Gamma_5\zeta | \mathcal{S}'_\theta | \Gamma_5\zeta \rangle = -1$, $\langle \Gamma_5\zeta | \mathcal{S}'_\epsilon | \Gamma_5\zeta \rangle = 0$), the eigenstates and eigenvalues of $\mathcal{H}_{eff}$ are obtained immediately from those of the appropriately displaced simple harmonic oscillators. Aside from a common shift of all the energy levels resulting from the linear Jahn-Teller term, which does not affect the relative spacing of the levels, the spectrum is given by

$$E = (n + \tfrac{1}{2})\hbar\omega' + (m + \tfrac{1}{2})\hbar\omega'' \ , \tag{A9}$$

with n, $m = 0, 1, 2, 3, \ldots$, and

$$\omega' = \omega_E^A[1 - \tfrac{54}{125}(E_{JT}^A/\zeta)]^{1/2}, \quad \text{(A10a)}$$

$$\omega'' = \omega_E^A[1 - \tfrac{27}{50}(E_{JT}^A/\zeta)]^{1/2}. \quad \text{(A10b)}$$

These frequencies are not only reduced as a result of the Jahn-Teller coupling to the higher spin-orbit states, but they differ slightly because of the presence in $\mathcal{H}_{eff}$ of the term involving $[\mathcal{E}_\theta'(Q_\epsilon^2 - Q_\theta^2) + \mathcal{E}_\epsilon'(2Q_\theta Q_\epsilon)]$, which has the form of a "quadratic Jahn-Teller coupling" and which thus serves to remove the "accidental" degeneracy of different states having a common value of $(n+m)$. Each vibronic level remains triply degenerate, however, and belongs either to Γ_4 or Γ_5. It may in fact be shown that all levels of Eq. (A9) for which m is odd belong to Γ_4, and all those for which m is even to Γ_5. These conclusions are, of course, consistent with the earlier results of Eq. (A4) when $(\hbar\omega)^2$ is neglected in the denominator of Eq. (A5) and the square root in Eq. (A10) is expanded. It must be noted, however, that our perturbation treatment would not be valid if the Jahn-Teller coupling were strong enough to make either argument under the square root in Eq. (A10) negative.

There is a second-order coupling, through the Jahn-Teller interaction, between the states $(\Gamma_5; \Gamma_5, J' = 1; 0_A, 1_B)$ and $(\Gamma_5; \Gamma_4, J' = 2; 1_A, 0_B)$ which may be important if the energy difference between these states is small (that is if $\hbar\omega_E^A + 2\zeta \simeq \hbar\omega_E^B$). This coupling contributes an off-diagonal term given by

$$w = \pm (\tfrac{3}{5})^{1/2}(E_{JT}^A E_{JT}^B \omega_E^A \omega_E^B)^{1/2}\hbar[-\tfrac{1}{5}(2\zeta + \hbar\omega_E^A)^{-1} + \tfrac{3}{10}(3\zeta - \hbar\omega_E^A)^{-1} + \tfrac{1}{2}(5\zeta + \hbar\omega_E^A)^{-1}] \quad \text{(A11)}$$

to the secular equation for these states, where the choice of sign in Eq. (A11) is the same as that of $(V_E^A V_E^B)$. The energies of the linear combinations of these two states that result from solving this secular equation (with neglect of coupling to other states) are then given [relative to the unperturbed energy of the Γ_5 $(J' = 1)$ ground state] by

$$E = \tfrac{1}{2}(u+v) \pm \tfrac{1}{2}[(u-v)^2 + 4w^2]^{1/2}, \quad \text{(A12)}$$

where we define

$$u = 2\zeta + \hbar\omega_E^A + \Delta E(\Gamma_5; \Gamma_4, J' = 2; 1_A, 0_B),$$

$$v = \hbar\omega_E^B + \Delta E(\Gamma_5; \Gamma_5, J' = 1; 0_A, 1_B),$$

as given by Eqs. (A4a) and (A6a).

Finally, we wish to determine the relative intensities of the vibronic sidebands that correspond to the excitation of one vibrational quantum and that result from the Jahn-Teller coupling, in both the ${}^5E \rightarrow {}^5T_2$ absorption spectrum and in the ${}^5T_2 \rightarrow {}^5E$ luminescence. Assuming for simplicity a negligibly small Jahn-Teller coupling in the ${}^5E$ state, we may evaluate these intensities for the absorption spectrum from the perturbation admixture of zero-phonon states into the one-phonon states, together with the appropriate electronic optical matrix elements (taken to be electric-dipole in T_d symmetry, as in Table X of SHC). For the emission spectrum, on the other hand, we must use the admixture of one-phonon states into the zero-phonon Γ_5 $(J' = 1)$ ground state [for simplicity we shall treat only the situation appropriate to 0 °K, for which the initial state in the absorption spectrum is the Γ_1 zero-phonon level of ${}^5E$, while all the luminescence is from the $(\Gamma_5; \Gamma_5, J' = 1; 0_A, 0_B)$ level of ${}^5T_2$]. We find in this way for the fraction f_a of the total integrated intensity of the ${}^5E \rightarrow {}^5T_2$ absorption spectrum which is transferred at 0 °K to each sideband corresponding to the Γ_5 states derived from the Γ_5 $(J' = 1)$ or Γ_4 $(J' = 2)$ electronic states by the excitation of one A quantum the results

$$f_a[(\Gamma_1, {}^5E) \rightarrow (\Gamma_5; \Gamma_5, J' = 1; 1_A, 0_B)] = \frac{1}{250}\frac{E_{JT}^A}{\hbar\omega_E^A}\left(\frac{9\hbar\omega_E^A}{5\zeta - \hbar\omega_E^A} - 1\right)^2, \quad \text{(A13)}$$

$$f_a[(\Gamma_1, {}^5E) \rightarrow (\Gamma_5; \Gamma_4, J' = 2; 1_A, 0_B)] = \frac{3}{50}\frac{E_{JT}^A}{\hbar\omega_E^A}\left(\frac{\hbar\omega_E^A}{2\zeta + \hbar\omega_E^A} + \frac{\hbar\omega_E^A}{3\zeta - \hbar\omega_E^A}\right)^2.$$

The corresponding result for the excitation of one B quantum is obtained by substituting B for A throughout Eq. (A13). For the ${}^5T_2 \rightarrow {}^5E$ luminescence at 0 °K the fraction $f_e(\Gamma_j, {}^5E; 1_A)$ of the total intensity transferred to each of the various one-quantum sidebands corresponding to the transition $(\Gamma_5; \Gamma_5, J' = 1; 0_A, 0_B) \rightarrow (\Gamma_j, {}^5E)$ with the excitation of one A phonon (for a B phonon replace A by B throughout) is found to be

$$f_e(\Gamma_1, {}^5E; 1_A) = \frac{1}{500}\frac{E_{JT}^A}{\hbar\omega_E^A}\left(\frac{9\hbar\omega_E^A}{5\zeta + \hbar\omega_E^A} + 1\right)^2,$$

$$f_e(\Gamma_2, {}^5E; 1_A) = \frac{1}{20}\frac{E_{JT}^A}{\hbar\omega_E^A}\left(\frac{\hbar\omega_E^A}{2\zeta + \hbar\omega_E^A} - \frac{\hbar\omega_E^A}{5\zeta + \hbar\omega_E^A}\right)^2,$$

$$f_e(\Gamma_3, {}^5E; 1_A) = f_e(\Gamma_1, {}^5E; 1_A) + f_e(\Gamma_2, {}^5E; 1_A), \quad \text{(A14)}$$

$$f_e(\Gamma_4, {}^5E; 1_A) = 3f_e(\Gamma_5, {}^5E; 1_A) = \frac{9}{2000}\frac{E_{JT}^A}{\hbar\omega_E^A}\left(\frac{6\hbar\omega_E^A}{5\zeta + \hbar\omega_E^A} - 1\right)^2 + \frac{3}{80}\frac{E_{JT}^A}{\hbar\omega_E^A}\left(\frac{\hbar\omega_E^A}{2\zeta + \hbar\omega_E^A} + \frac{2\hbar\omega_E^A}{5\zeta + \hbar\omega_E^A}\right)^2.$$

[1]G. A. Slack, F. S. Ham, and R. M. Chrenko, Phys. Rev. 152, 376 (1966). This paper will be referred to as SHC.

[2]G. A. Slack and B. M. O'Meara, Phys. Rev. 163, 335 (1967).

[3]F. S. Ham, Phys. Rev. 138, A1727 (1965).

[4]C. H. Henry, S. E. Schnatterly, and C. P. Slichter, Phys. Rev. 137, A583 (1965).

[5]M. D. Sturge, in *Solid State Physics*, edited by F. Seitz, D. Turnbull, and H. Ehrenreich (Academic, New York, 1967), Vol. 20, p. 91.

[6]Y. Toyozawa and M. Inoue, J. Phys. Soc. Japan 21, 1663 (1966).

[7]F. S. Ham, W. M. Schwarz, and M. C. M. O'Brien, Phys. Rev. 185, 548 (1969).

[8]P. J. Stephens and M. Lowe-Pariseau, Phys. Rev. 171, 322 (1968); M. D. Sturge, Phys. Rev. B 1, 1005 (1970); A. E. Hughes, J. Phys. C 3, 627 (1970).

[9]Origin of vibronic sidebands in electronic spectra has been discussed in many papers, for example, by D. S. McClure and M. H. L. Pryce, in *Phonons in Perfect Lattices and in Lattices with Point Imperfections*, edited by R. W. H. Stevenson (Plenum, New York, 1966), pp. 310 and 403; A. A. Maradudin, in *Solid State Physics*, edited by F. Seitz and D. Turnbull (Academic, New York, 1966), Vol. 18, p. 274; M. Wagner, Physik Kondensierten Materie 4, 71 (1965); G. Herzberg, *Molecular Spectra and Molecular Structure III. Electronic Spectra and Electronic Structure of Polyatomic Molecules* (Van Nostrand, Princeton, N. J., 1966), pp. 142–183.

[10]W. Moffitt and A. D. Liehr, Phys. Rev. 106, 1195 (1957).

[11]W. Moffitt and W. Thorson, Phys. Rev. 108, 1251 (1957).

[12]H. C. Longuet-Higgins, U. Opik, M. H. L. Pryce, and R. A. Sack, Proc. Roy. Soc. (London) A244, 1 (1958).

[13]B. Weinstock and G. L. Goodman, in *Advances in Chemical Physics*, edited by I. Prigogine (Interscience, New York, 1965), Vol. 9, p. 169.

[14]G. Herzberg, *Molecular Spectra and Molecular Structure III. Electronic Spectra and Electronic Structure of Polyatomic Molecules* (Van Nostrand, Princeton, N. J., 1966), pp. 54–61.

[15]G. A. Slack, S. Roberts, and J. T. Vallin, Phys. Rev. 187, 511 (1969).

[16]J. M. Baranowski, J. W. Allen, and G. L. Pearson, Phys. Rev. 160, 627 (1967).

[17]J. J. Haanstra, in *II-VI Semiconducting Compounds*, edited by D. G. Thomas (Benjamin, New York, 1967), p. 207.

[18]Levels of ^5E are numbered 1–5 as in SHC (Ref. 1), while the irreducible representations of the point group T_d to which the various spin-orbit levels belong are labeled using Bethe's notation [H. A. Bethe, Ann. Physik 3, 133 (1929)], as in the tables of Koster *et al.* (Ref. 33, p. 88).

[19]M. H. L. Pryce, Phys. Rev. 80, 1107 (1950).

[20]*Atomic Energy Levels*, edited by C. E. Moore (U. S. GPO, Washington, D. C., 1952), Vol. 2, p. 60.

[21]G. A. Slack, S. Roberts, and F. S. Ham, Phys. Rev. 155, 170 (1967); J. T. Vallin, G. A. Slack, and C. C. Bradley, Phys. Rev. B 2, 4406 (1970).

[22]J. P. Mahoney, C. C. Lin, W. H. Brumage, and F. Dorman, J. Chem. Phys. 53, 4286 (1970).

[23]Because most of the peaks in absorption and luminescence spectra of Fe^{2+} in ZnS in near infrared have oscillator strengths too large to be attributed to magnetic dipole processes (see Ref. 1), we will ignore such processes in the discussion in this paper.

[24]See Table V of SHC (Ref. 1) and references cited therein.

[25]O. Brafman and S. S. Mitra, Phys. Rev. 171, 931 (1968).

[26]W. G. Nilsen, Phys. Rev. 182, 838 (1969).

[27]L. Merten, Z. Naturforsch. 13a, 662 (1958); 13a, 1067 (1958).

[28]A. K. Rajagopal and R. Srinivasan, Z. Physik 158, 471 (1960).

[29]J. F. Vetelino, S. S. Mitra, O. Brafman, and T. C. Damen, Solid State Commun. 7, 1809 (1969).

[30]J. Bergsma, Phys. Letters 32A, 324 (1970).

[31]L. A. Feldkamp, G. Venkataraman, and J. S. King, Solid State Commun. 7, 1571 (1969).

[32]R. Loudon, Proc. Phys. Soc. (London) 84, 379 (1964).

[33]G. F. Koster, J. O. Dimmock, R. G. Wheeler, and H. Statz, *Properties of the Thirty-Two Point Groups* (MIT U. P., Cambridge, Mass., 1963).

[34]J. H. Van Vleck, J. Chem. Phys. 7, 72 (1939); U. Opik and M. H. L. Pryce, Proc. Roy. Soc. (London) A238, 425 (1957).

[35]We use subscripts θ and ϵ to label operators belonging as partners to Γ_3 and transforming, respectively, as $[2z^2-(x^2+y^2)]$ and $\sqrt{3}(x^2-y^2)$, and the subscripts ξ, η, and ζ for those belonging to Γ_5 and transforming as yz, zx, and xy or equivalently (under T_d) as x, y, and z.

[36]K. Huang and A. Rhys, Proc. Roy. Soc. (London) A204, 406 (1950).

[37]If a local mode has a substantial frequency difference between the initial and final states, then as shown by T. Miyakawa and S. Oyama [Phys. Letters 28A, 206 (1968)] the distribution of sideband intensity may depart significantly from the Poisson distribution of Eq. (9). In particular, this distribution would then be different in the absorption and emission spectra, and the sidebands would extend to higher n in the transition in which the final state has the larger vibrational frequency. However, there is no possible choice for the parameters in such a model that could account for *strong* sidebands with $n=2$ and 3 in one transition [as supposed in Table VI of SHC, Ref. 1] while allowing only the $n=0$ and 1 peaks to be strong in the reverse transition.

[38]This case exhibits the various effects of Jahn-Teller coupling which we wish to emphasize, while its analysis is much simpler algebraically than it would be if coupling with a Γ_5 mode were included. Moreover, Γ_3 coupling may very well be the dominant Jahn-Teller interaction in the $^5T_2$ state of tetrahedrally coordinated Fe^{2+} since the $^5T_2$ state of Cr^{2+} has been found (Ref. 58) to suffer a static Jahn-Teller distortion in ZnSe, ZnTe, and some other II-VI compounds as a result of interaction with a Γ_3 mode. Nevertheless, we do not wish to imply that we can rule out the possibility that one or more Γ_5 modes may make important contributions to Jahn-Teller coupling for the $^5T_2$ state of Fe^{2+}.

[39]Comparison of the calculated points with the lines in Fig. 2 shows the fairly good accuracy of the perturbation results for the $\Gamma_5(J'=1)$ and Γ_3, $\Gamma_4(J'=2)$ levels for E^B_{JT} as large as $\sim 2\zeta = 200$ cm^{-1}, but the greatly diminished accuracy for levels with one (or more) vibrational quan-

tum excited. Nevertheless, the qualitative trends of the levels and their relative displacements as a function of E_{JT}^B are given quite satisfactorily by the perturbation results. Similar accuracy is to be expected in the other cases we have treated, for which we have obtained only perturbation results.

[40]The Γ_3 ($J'=2$) state gives rise to one-phonon levels belonging to Γ_1, Γ_2, and Γ_3, with which we shall not be concerned. We have also not included in Fig. 3 any of the two- or three-phonon levels derived from Γ_5 ($J'=1$), which have energies within range of the figure.

[41]See also Fig. 1(b) of Ref. 7. As expected, this lowest group contains two Γ_4, two Γ_5, and one Γ_3 states in addition to one Γ_1 state not shown.

[42]Effective spin Hamiltonian in the $^5T_2$ state for a static Jahn-Teller distortion along z axis would be DS_z^2, where D should be given in terms of parameters of Sec. II (for $\Delta \gg 3E_{JT}$) by

$$D=\lambda^2/3E_{JT}+4\lambda^2/\Delta-3\rho,$$

the sign of the second term corresponding to that of having $^5T_2$ *above* ^5E. Assuming $D>0$, we would then have that the lowest vibronic spin-orbit level of Figs. 2–4 remains the Γ_5 level ($S_z=0$) even in the static Jahn-Teller limit. The levels corresponding to $S_z=\pm1$ in the limit are Γ_4 and Γ_5, while levels corresponding to $S_z=\pm2$ are Γ_1, Γ_3, and Γ_4. [If $^5T_2$ is *below* ^5E, D can have either sign, as Vallin and Watkins (Ref. 58) have, in fact, found for Cr^{2+} in tetrahedral coordination. If D is negative, the Γ_5 level then does *not* remain the ground state in the static limit.]

[43]J. Vallin, Phys. Rev. B 2, 2390 (1970).

[44]A small departure from a uniform spacing of the levels in zero magnetic field was indicated by data of Ref. 22. However, as shown in Table IV of Ref. 15, such small departures from uniformity may result from spin-orbit interaction when it is treated to higher accuracy than to second order in (λ/Δ), as well as from the Jahn-Teller coupling.

[45]F. S. Ham, Phys. Rev. 166, 307 (1968).

[46]F. S. Ham, in *Electron Paramagnetic Resonance*, edited by S. Geschwind (Plenum, New York, 1971).

[47]M. Wagner, J. Chem. Phys. 41, 3939 (1964).

[48]A large frequency shift between the ground and excited states of Eu^{2+} in NaCl, KCl, and RbCl has been inferred by W. Bron and M. Wagner [Phys. Rev. 145, 689 (1966)] for an odd mode involved in a "pseudo-Jahn-Teller coupling," between nearly degenerate states of opposite parity from $4f^7$ and $4f^65d$ electronic configurations of Eu^{2+}. The large frequency shift in this case is the result of close proximity of these electronic levels.

[49]R. G. Pearson, J. Am. Chem. Soc. 91, 1252 (1967); 91, 4947 (1967); J. Chem. Phys. 52, 2167 (1970).

[50]S. A. Kazanskii, A. I. Ryskin, and G. I. Khilko, Opt. i Spektroskopiya 27, 296 (1969) [Opt. Spectry. (USSR) 27, 156 (1969)].

[51]G. A. Slack and S. Roberts, Phys. Rev. B 3, 2613 (1971).

[52]G. Herzberg and E. Teller, Z. Physik. Chem. B21, 410 (1933).

[53]H. Sponer and E. Teller, Rev. Mod. Phys. 13, 75 (1941).

[54]L. E. Orgel, J. Chem. Phys. 23, 1824 (1955).

[55]J. H. Van Vleck, J. Phys. Chem. 41, 67 (1937).

[56]A. D. Liehr and C. J. Ballhausen, Phys. Rev. 106, 1161 (1957).

[57]R. A. Satten, J. Chem. Phys. 27, 286 (1957); 29, 658 (1958).

[58]J. T. Vallin and G. D. Watkins, Solid State Commun. (to be published).

[59]As a consequence, the value $Dq=-340$ cm^{-1} obtained from this ratio by SHC is not changed in our revised interpretation.

[60]If V_AQ_A represents the difference in the linear coupling of the ^5E and $^5T_2$ states to a Γ_1 mode, as given by Eq. (5), we have $\Delta E_A=V_A^2/2\mu_A\omega_A^2$ and $S_A=E_A/\hbar\omega_A$. For a Γ_5 mode to which coupling is given in Eq. (7), we have (Ref. 7) $(E_{JT})_T=2V_T^2/3\mu_T\omega_T^2$ and $S_T=(E_{JT})_T/\hbar\omega_T$.

[61]See Table VI in Ref. 1.

[62]M. C. M. O'Brien, Proc. Phys. Soc. (London) 86, 847 (1965).

[63]P. R. Moran, Phys. Rev. 137, A1016 (1965).

[64]K. Cho, J. Phys. Soc. Japan 25, 1372 (1968).

[65]R. Englman, M. Caner, and S. Toaff, J. Phys. Soc. Japan 29, 306 (1970).

[66]H. R. Fetterman and D. B. Fitchen, Solid State Commun. 6, 501 (1968).

[67]J. A. Davis and D. B. Fitchen, Solid State Commun. 6, 505 (1968); J. A. Davis, Ph. D. thesis (Cornell University, 1970) (unpublished).

[68]Y. Merle d'Aubigné and A. Roussel Phys. Rev. B 3, 1421 (1971).

[69]See Sec. II in Ref. 7.

[70]We label vibronic eigenstates of $\mathcal{H}_0$ [as on the left-hand side of Eq. (A3)] by, first, the irreducible representation of T_d to which the over-all state belongs (taking account of transformational behavior of both electronic and vibrational parts of the wave function), then the electronic state of $^5T_2$ from which the vibronic state derives, and finally the number of quanta N_A and N_B of each type A and B which characterizes vibrational excitation of the state. Unperturbed energy of this vibronic state thus lies $(N_A\hbar\omega_E^A+N_B\hbar\omega_E^B)$ above the energy of the corresponding electronic state as given by Fig. 1. (For levels with $N_A+N_B>1$ this notation does not suffice to distinguish all the vibronic states, but, except as noted, we shall not be concerned with these levels.)